A PERSONAL OVERVIEW OF THE DEVELOPMENT OF PATCH ANTENNAS

Part 3

Kai Fong Lee

Dean Emeritus, School of Engineering and Professor Emeritus, Electrical Engineering, University of Mississippi

and

Professor Emeritus, Electrical Engineering, University of Missouri-Columbia

November 4, 2015

City University of Hong Kong

Schedule

Part 1 (Hour 1)	Part 2 (Hour 2)	Part 3 (Hour 3)	Part 4 (Hour 4)
1. How I got into patch antenna research 2. Basic geometry and basic characteristics of patch antennas 3. Our first topic 4. Our research on topics related to basic studies	5. Broadbanding techniques 6. Full wave analysis and CAD formulas	7. Dual/triple band designs 8. Designs for circular polarization	9. Reconfigurable patch antennas 10. Size reduction techniques 11. Concluding remarks and some citation data

7. DUAL/TRIPLE-BAND DESIGNS

7.1 Introductory Remarks

- There are many applications in wireless communications that involves two distinct frequencies. Because of the attractive features of the microstrip patch antenna, such as planar profile, ruggedness and low cost, there has been considerable interest in the development of these antennas to meet dual –frequency specifications. It is sometimes possible that a broadband microstrip antenna can cover the frequencies of interest. However, the disadvantage of using a broadband antenna is that it also receives non-desired frequencies unless some kind of filtering network is introduced to reject such frequencies. On the other hand, the advantage of a dual-frequency designs is that it focuses only on the frequencies of interest and is thus more desirable.
- The above remark can be extended to more than two frequencies.
- There are many dual/multiple designs developed. In what follows, we will describe several of them. Some are left out because of time limitation.

7.2 Stacked Patches
7.2.1 Dual-Band Stacked Patches

- Previously, stacked patches were introduced for broadband designs. In that application, the bottom patch was fed while the upper patch was parasitic. This produced strong coupling between the two resonances of the patches, resulting in broadband behavior.
- Stacked patches can also be designed for dual-frequency operation. For the coax-fed case, the center conduction passes through a clearance hole in the lower patch and is connected directly to the upper patch, as shown in Fig. 1. Such an arrangement appears to result in a weak coupling of the two resonances of the two patches, leading to dual-frequency operation.

7.2.1 Dual-Band Stacked Patches

- The first experimental study of such a design was reported by Long and Walton [1979]. Two stacked circular patches (Fig.3.1) were photo-etched on separate substrates and aligned so that their centers were along the same line. The sizes of the two discs and their spacings were varied and the resultant antenna characteristics measured. If one considers the two regions under the patch as two resonant cavities it is clear that the system behaves as a pair of coupled cavities. Since the fringing fields are different for the upper and lower cavities, two resonant frequencies are expected even if the diameters of the two discs are the same.
- Figure 3.2 shows the measured real and imaginary parts of the input impedance for $2a_2$=3.78 cm, t_1= t_2=0.075 cm and three values of $2a_1$ [Long and Walton, 1979].

7.2.1 Dual-Band Stacked Patches

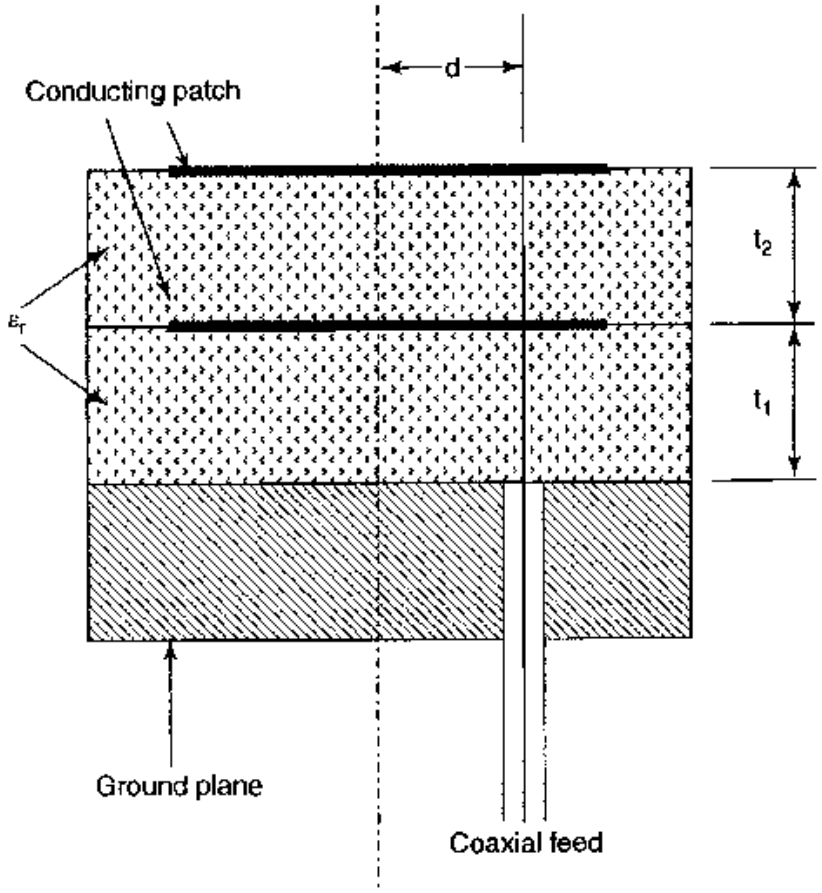

Fig.3.1. Dual-frequency stacked microstrip antenna.

7.2.1 Dual-Band Stacked Patches

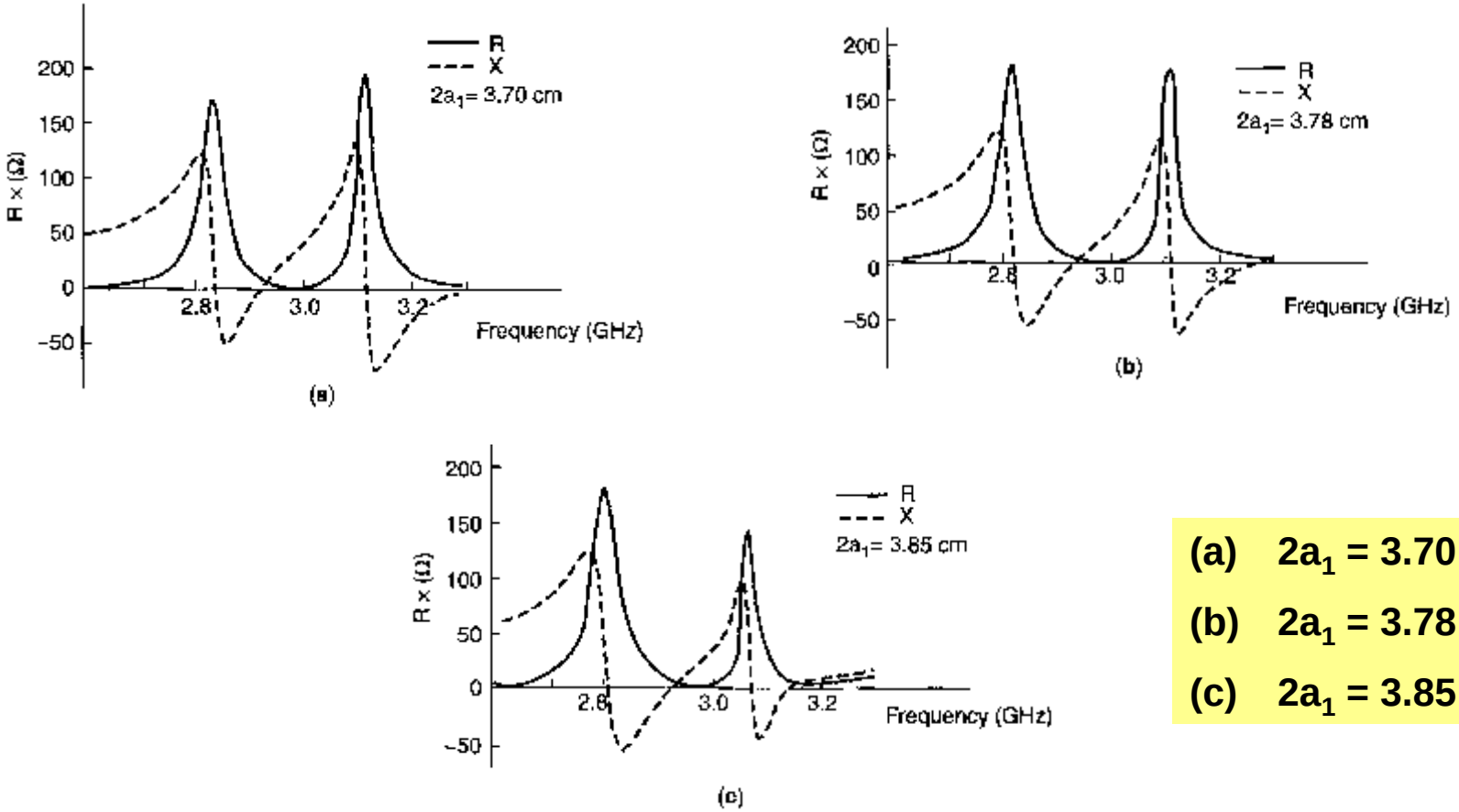

(a) $2a_1 = 3.70$ cm

(b) $2a_1 = 3.78$ cm

(c) $2a_1 = 3.85$ cm

Fig. 3.2 Real and imaginary parts of impedance of stacked circular patches stacked on a dielectric with $\varepsilon_r = 2.47$.

7.2.1 Dual-Band Stacked Patches

- Figure 3.3 shows the resonant frequencies as a function of the upper disc parameter. Also shown is the resonant frequency of the lowest mode of a single disc of diameter $2a_1$ and substrate thickness t = 0.075 cm, taking into account the fringing field through the effective diameter. It is seen that the lower resonant frequency is relatively constant. The upper resonance, on the other hand, is highly dependent on the size of the upper disc.
- Radiation patterns were also taken by Long and Walton and were shown in Fig. 4. They were similar to the radiation patterns of the lowest mode for the single circular patch.

7.2.1 Dual-Band Stacked Patches

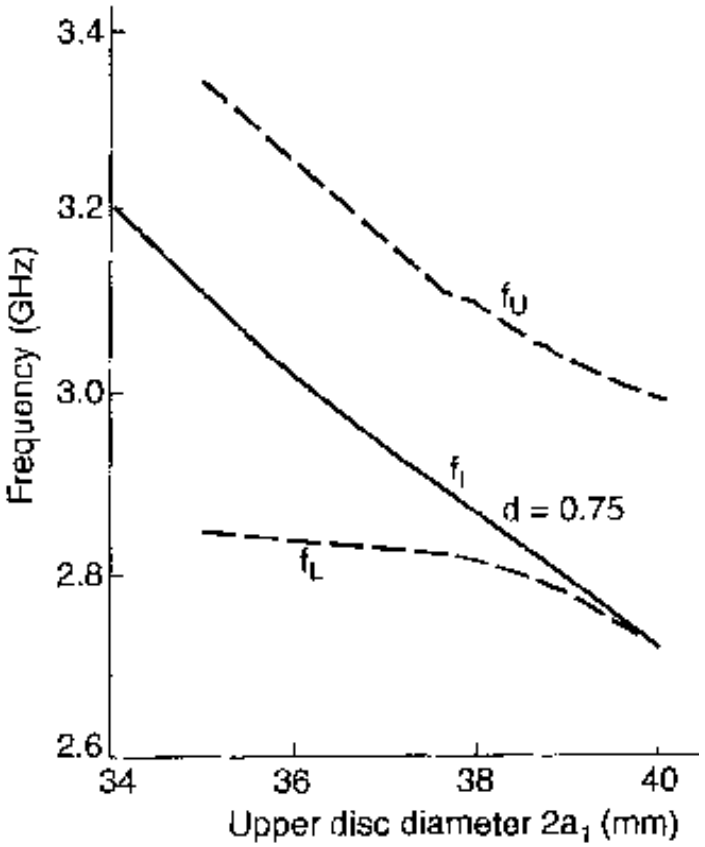

Fig. 3.3 Resonant frequencies versus upper disc diameter of stacked circular patches etched on a dielectric with $\varepsilon_r = 2.47$, $2a_2 = 3.78$ cm, $t_1 = t_2 = 0.75$ mm.

7.2.1 Dual-Band Stacked Patches

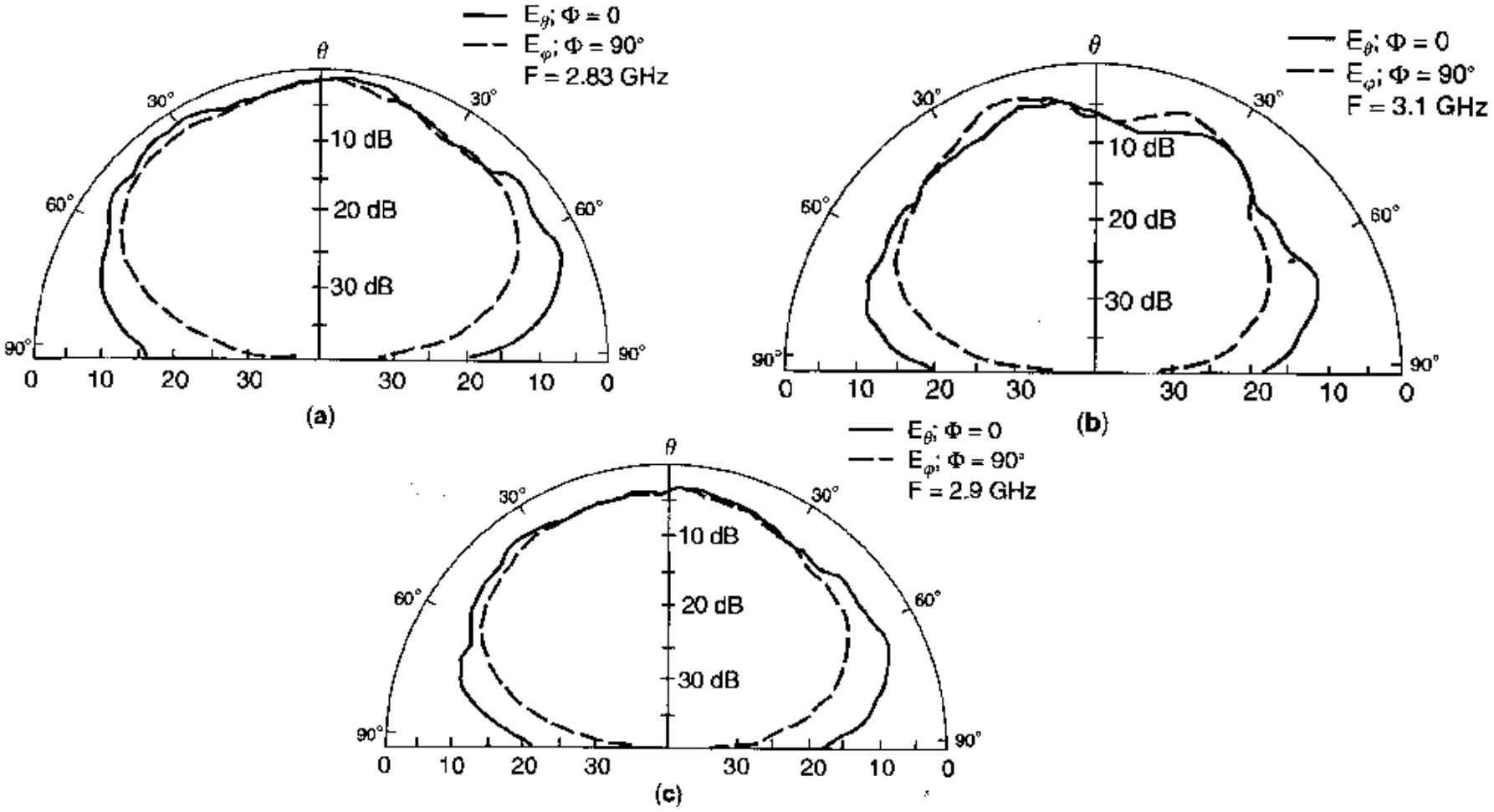

Fig. 3.4 Radiation patterns of stacked circular-disc antenna. (a) *f* = 2.83 GHz, (b) *f* = 3.1 GHz, (c) *f* = 2.9 GHz.

7.2.2 Multi-Band Stacked Patches

- It is clear that the technique of using stacked patches for dual band operation can be extended to multi-bands by simply stacking patches in multi-layers. As an example, Fig.3.5 shows an antenna consisting of a driven patch and four parasitic patches placed underneath the driven patch [J. Anguera et al. 2003].

- The driven patch, which has dimensions of 51x51 mm, was fed by a coaxial probe through an etched capacitor in order to mitigate the mismatching due to the probe inductance. The driven patch was etched on a thin substrate of h=0.8 mm and ε_r =3.38. The parasitic patches are separated and supported by foam substrate with ε_r =1.07 and are slightly larger than the driven patch. The inner conductor of the coaxial probe went through a 2 mm diameter hole in each of the parasitic patches with no physical contact. The total antenna height was 15.6 mm and the ground plane dimensions were 220x180 mm.

7.2.2 Multi-Band Stacked Patches

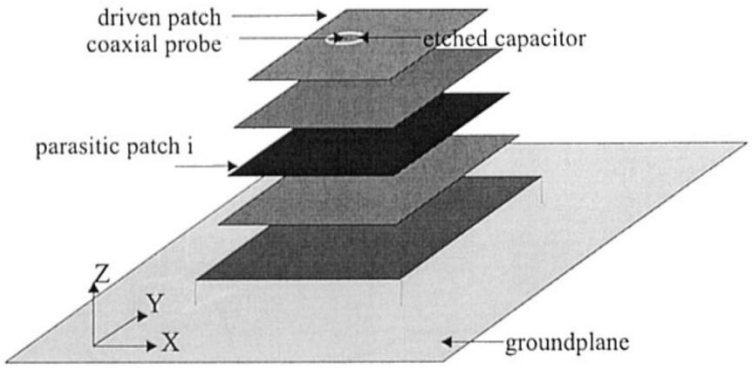

(a) Pictorial View

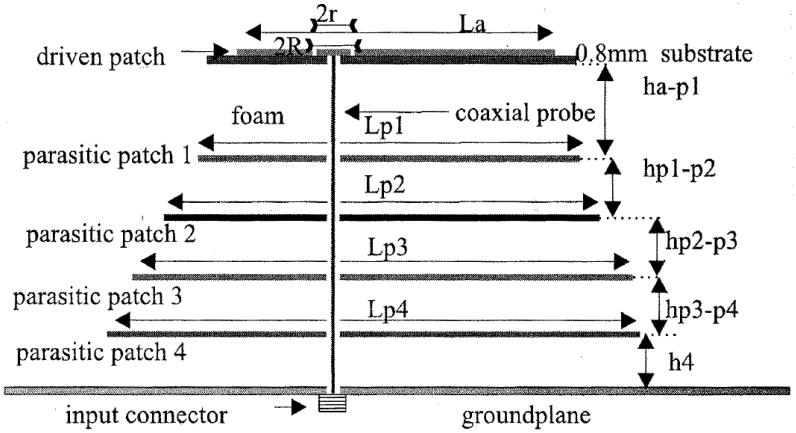

(b) Side view and dimensions

Fig.3.5 Multi-band stacked patches

All patches are square-shaped. La=51, Lp1=65, Lp2=70, Lp3=75, Lp4=80, ha-p1=6, hp1-p2=2, hp2-p3=2, hp3-p4=2, h4=2. Inner radius of the etched capacitor r=3.6; outer radius R=4.7. Feeding point is placed 13mm from the driven patch center. Patch centers are aligned. All dimensions are in millimeters.

7.2.2 Multi-Band Stacked Patches

Table 3.1 BW and Gain experimental results

Band	f_o/GHz	BW(SWR=2)/%	Gain/dB	f_i/f_o
1	1.634	5.5	9.2	-
2	1.819	2.0	8.4	1.113
3	1.954	2.7	7.6	1.195
4	2.092	1.5	6.9	1.280
5	2.289	5.3	7.3	1.4

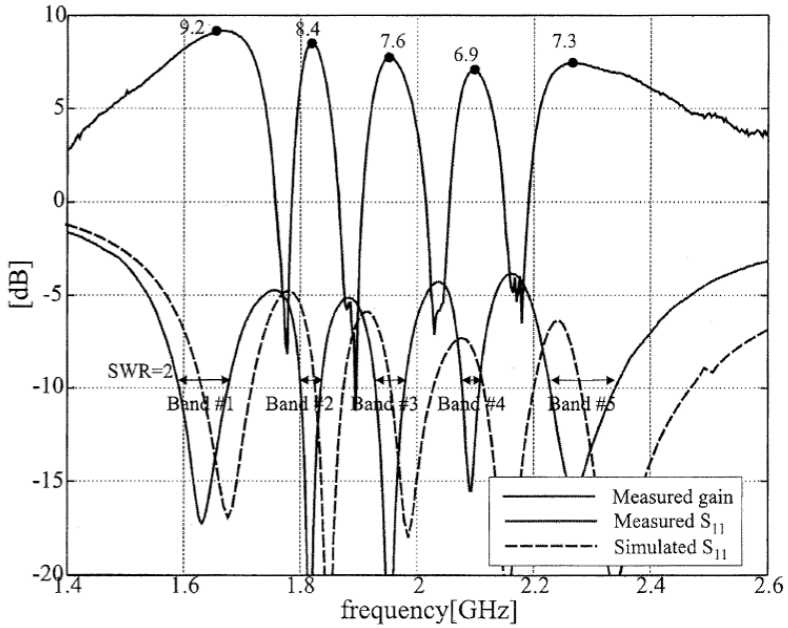

Fig.3.6 Measured/simulated return loss and measured gain (θ=0°)

7.2.2 Multi-Band Stacked Patches

- Measured results of the antenna are listed in Table 3.1. Fig.3.6 shows the measured frequency responses of gain and return loss, as well as the simulated return loss. It is seen that the antenna could be operated at five frequency bands with gains varying from 7 to 9 dB, and bandwidth varying from 1.5% to 5.5%. The operating bands are closely packed in this design (small-frequency ratios). The simulated radiation patterns (not shown) are found to be similar and stable at the five bands.

7.3 Use of Dual-Modes in Rectangular Patch

- In the stacked patch design for dual band, the frequency ratio of the two bands is small, usually less than 1.5.
- If for a particular patch shape two modes can be found which produce similar radiation patterns with the same polarization, dual frequency is possible with a single patch. For the rectangular patch, the two modes TM_{01} and TM_{03} satisfy this requirement, as are the TM_{10} and TM_{30} modes. However, their resonant frequencies are related by a ratio of approximately 3, the exact value being dependent on the edge effect.
- It has been shown that, by placing shorting pins on the nodal lines of the TM_{03} mode field, it has little effect on this mode but a strong effect on the TM_{01} mode.
- Zhong and Lo [1983] demonstrated that this offered a way of altering not only the separation of the two frequency bands but also the input impedance of the TM_{01} mode as well. The geometry of the rectangular patch in their experiments is shown in Fig. 3.7. It is made of 1/8 in copper-cladded Rexolite 2200 with six shorting-pin positions.

7.3 Use of Dual-Modes in Rectangular Patch

- The effects of successively adding more and more pins (each approximately 0.05 cm in diameter) at the positions indicated in Fig. 3.7 are shown in Table 3.2. It is seen that the ratio of the two operating frequencies f_{03}/f_{01} can be varied approximately from 3 to 2. Since all these pins are located on the TM_{03} mode null lines, f_{03} remains constant at about 1865 MHz while f_{01} is varied from 613 to 891 MHz. In order for the impedance of the two bands to be close to 50 Ω at resonance it is necessary to attach a short capacitive stub of 0.6 cm $\times$ 2.1 cm. With the stub added, the bandwidth with references to 3:1 SWR is about 2 % for the low band and almost 8 % for the high band. Typical low-and high-band patterns in both E and H planes are shown in Fig. 9. It is seen that, while the two modes radiate strongest in the broadside, the directivities of the two modes are quite different.

7.3 Use of Dual-Modes in Rectangular Patch

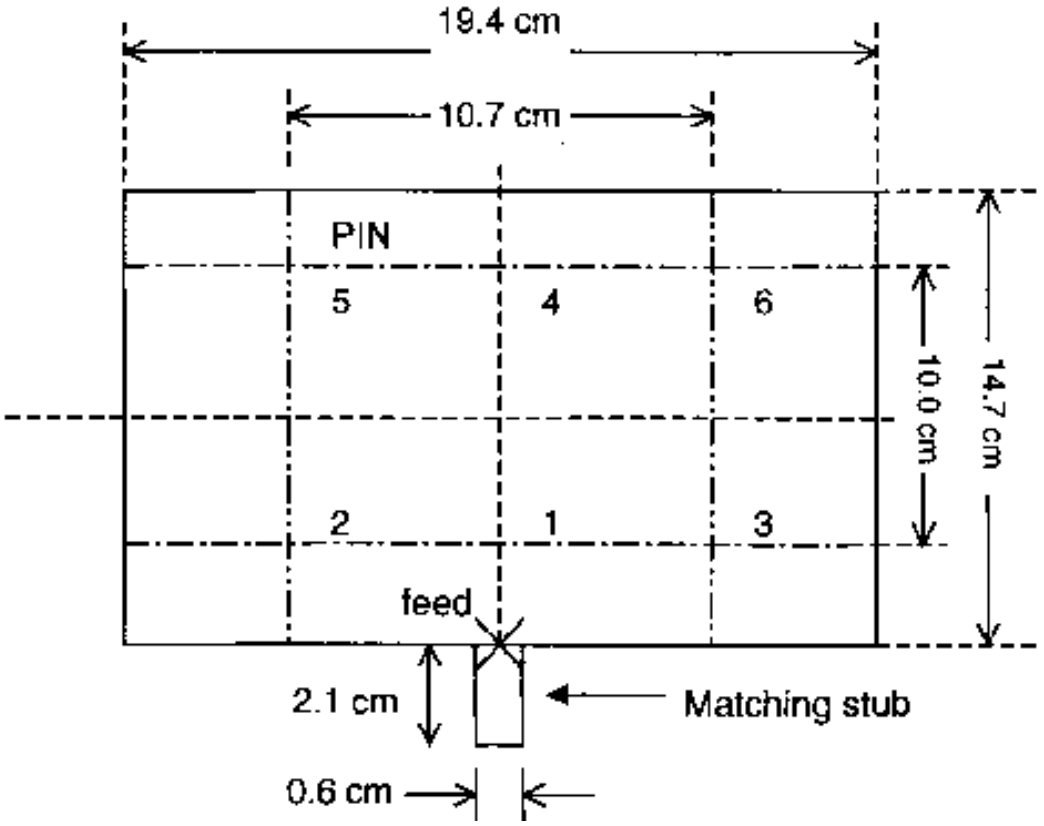

Fig. 3.7 Geometry of a rectangular patch antenna with six possible shorting pins and a short match stub.

7.3 Use of Dual-Modes in Rectangular Patch

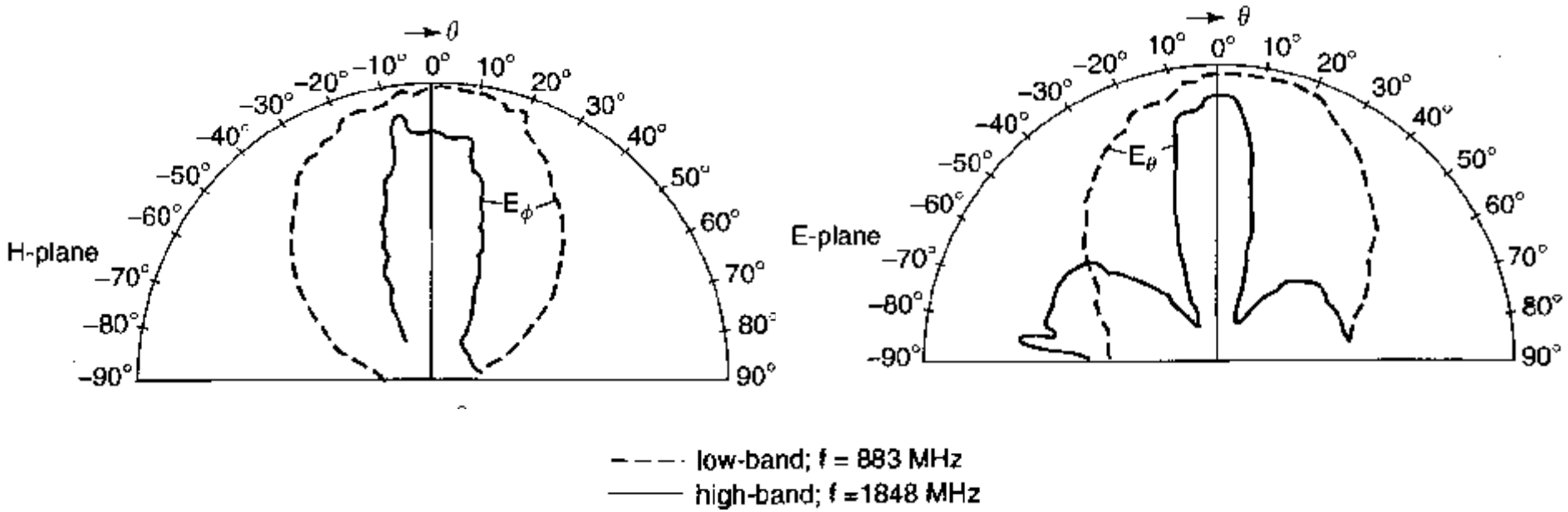

Fig. 3.8 Typical radiation patterns in H- and E-planes for antennas shown in Fig. 14.8 with six pins inserted.

7.3 Use of Dual-Modes in Rectangular Patch

Table 3.2 Resonant frequencies of the TM_{01} and TM_{03} modes against shorting pins u

Number of Pins	Pin Position	f_{01} (MHz)	f_{03} (MHz)	f_{03}/f_{01}
0	–	613	1861	3.04
1	(1)	664	1874	2.82
2	(1)(2)	706	1865	2.64
3	(1)(2)(3)	792	1865	2.36
4	(1)(2)(3)(6)	813	1865	2.29
5	(1)(2)(3)(5)(6)	846	1865	2.20
6	(1) to (6)	891	1865	2.09

- A dual-band rectangular patch antenna with a frequency ratio less than 2 can also be obtained by loading the patch with two narrow slots etched inside the patch, as shown in Fig.3.9. Maci (1995) demonstrated that, if the slots were placed at locations where the current of the lower mode is near minimum while the current for the unperturbed higher mode is significant, the resonant frequency of the lower mode is not much affected while that of the upper mode is decreased. In his experiment, the frequency ratio was reduced to 1.89 from the original 3.0

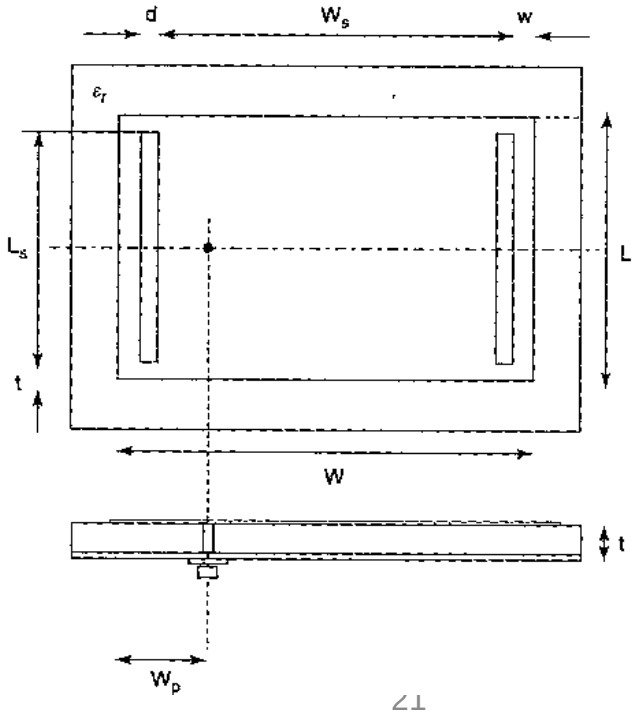

Fig. 3.9 Geometry of probe feed Slot-loaded patch antenna.

References for dual/multiple band stacked patches and use of dual modes

S. A. Long and W. D. Walton, “A dual frequency stacked circular disk antenna,” IEEE Transactions on Antennas and Propag., Vol. 27, 270-273, 1979.

J. S. Dahele, K. F. Lee, and D.P. Wong, Dual-frequency stacked annular-ring microstrip antenna, IEEE Trans. on Antennas and Propag., AP-35, pp. 1281-1285, 1987.

Z. Fan and K. F. Lee, Hankel transform domain analysis of dual-frequency stacked circular-disk and annular-ring microstrip antennas, IEEE Trans. on Antennas and Propag., AP-39, pp. 867-870, 1991.

J. Anguera, G. Font, C. Puente, C. Borja and J. Soler, Multifreequency microstrip patch antenna using multiple stacked elements, IEEE Microwave and Wirless Component Letters, Vol. 13, pp. 123-124, 2003.

S. S. Zhong and Y. T. Lo, “Single-element rectangular microstrip antenna for dual-frequency operation,” Electronics Letters, Vol. 19, pp. 298-300, 1983.

S. Maci, G. Biffi Gentili, P. Piazzesi, and C. Salvador, “Dual band slot loaded patch antenna,” IEE Proc. Microwaves Antennas Propag. H, Vol. 142, pp. 225-232, 1995.

K. M. Luk, C. H. Lai and K. F. Lee, “Wideband L-probe-feed antenna with dual-band operation for GSM/PCS base stations,” Electronics Letters, Vol. 35, pp. 1123-1124, 1999.

7.4. Use of U-Slots in Dual/Triple-Band Operations

7.4.1 Introductory remarks

- It was pointed out in Lee et al. (1997) that, in addition to broadbanding, U-slots can also be used to design dual band patch antennas. This was later expanded to include triple band. There are two situations: large frequency ratio (>1.5) and small frequency ratio (<1.5).

- In the large frequency ratio case, the patch dimension determines one resonance, while the slot dimensions provide the additional resonances.

- In the small frequency ratio case, one starts with a broadband patch antenna, such as a L-probe fed patch, U-slot patch, M-probe fed patch, coaxial-fed or aperture coupled stacked patches.

- U-slots are then cut in the patch to introduce band notches. The band notches occur at frequencies determined by the dimensions of the U-slots.

- If one U-slot is cut, a dual band antenna results. If two U-slots are cut, a triple band antenna results. The U-slots act as anti-resonances in these applications.

7.4.2 Large frequency ratio designs

7.4.2.1 Example of Dual Band Design

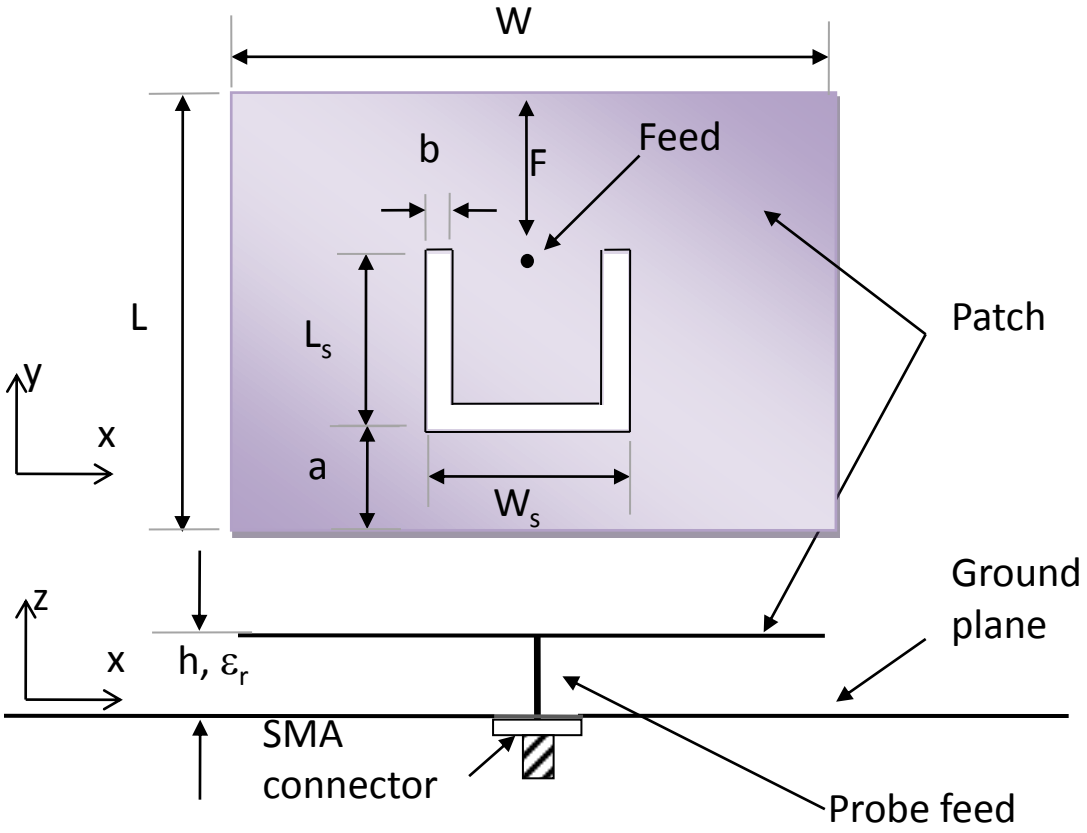

Fig.3.10 Geometry dual band U-slot patch antenna

Dual band

Dimensions	
W	64mm
L	54mm
F	28.4mm
W_s	34mm
L_s	22mm
a	8.4mm
b	11mm
h	6mm

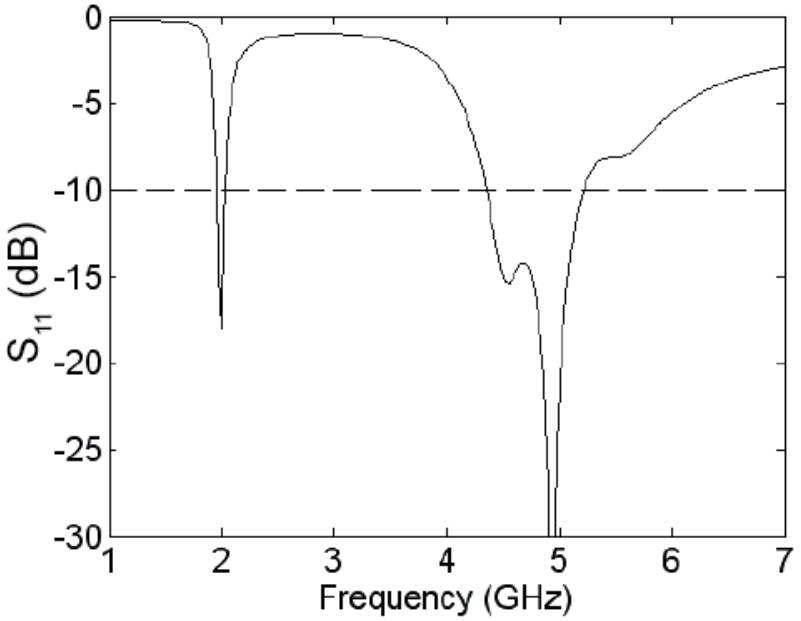

Fig. 3.11 The impedance bandwidths at the lower and upper bands are 3.5% and 18.2% respectively.

7.4.2.2 Example of triple band design

Dimensions	
W	64mm
L	54mm
F	28.4mm
W_U	34mm
L_U	22mm
W_H	28mm
L_H	13.5mm
a	8.4mm
b	11mm
c	1.5mm
d	2mm
h	6mm

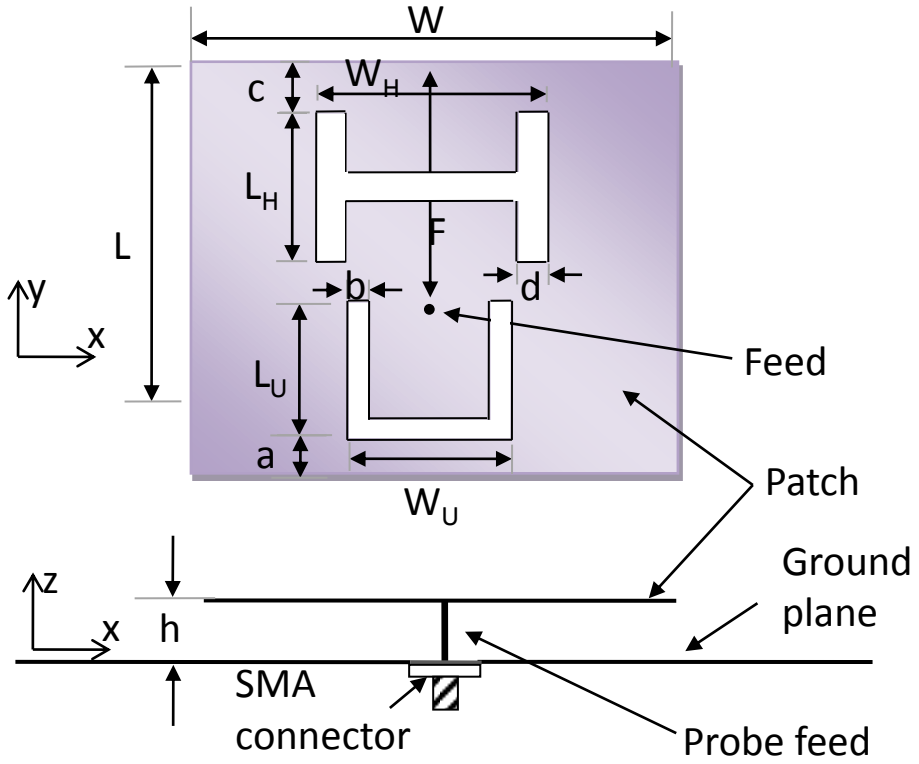

Fig. 3.12 Geometry of triple band U-slot patch antenna

Fig.3.13 The impedance bandwidths at the three bands are 2.6% for the lower band (@1.94 GHz), 9.8% for the middle band (@4.16 GHz), and 10.4% for the upper band (@5.44 GHz).

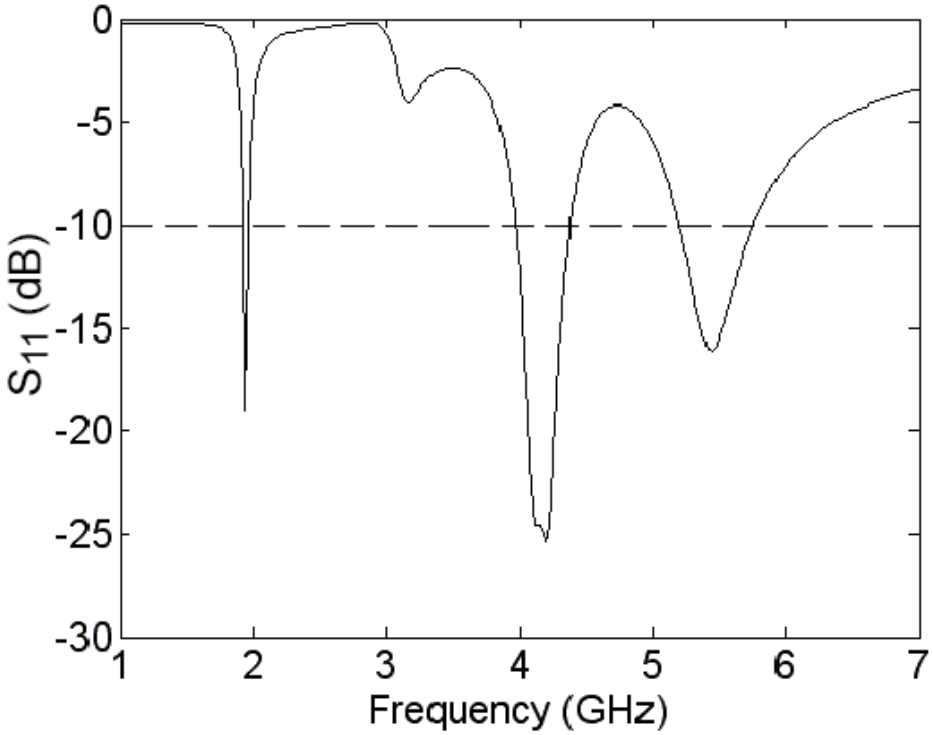

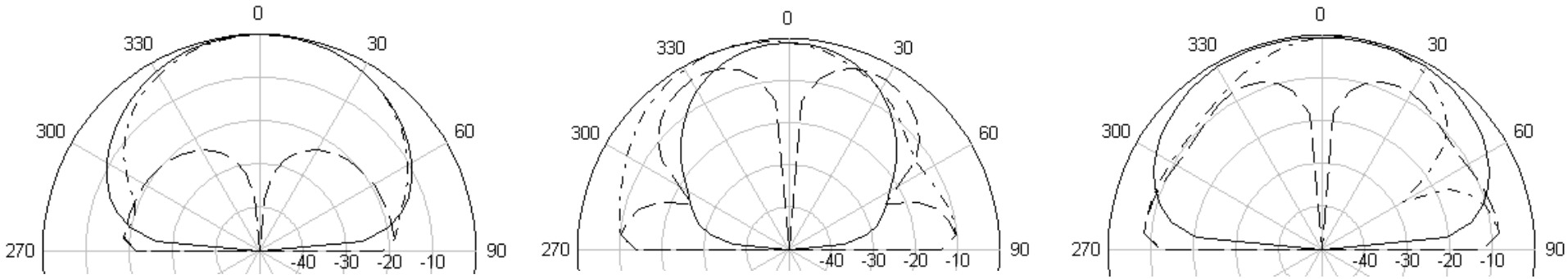

Fig. 3.14 Simulated radiation pattern of the triple-band U-slot antenna at (a) 1.94 GHz, (b) 4.16 GHz, and (c) 5.44 GHz.

(——— H-Co, – – – – H-x, – · – · – · E-Co)

7.4.3 Small frequency ratio designs

7.4.3.1 Starting with the L-Probe Fed Broadband Patch

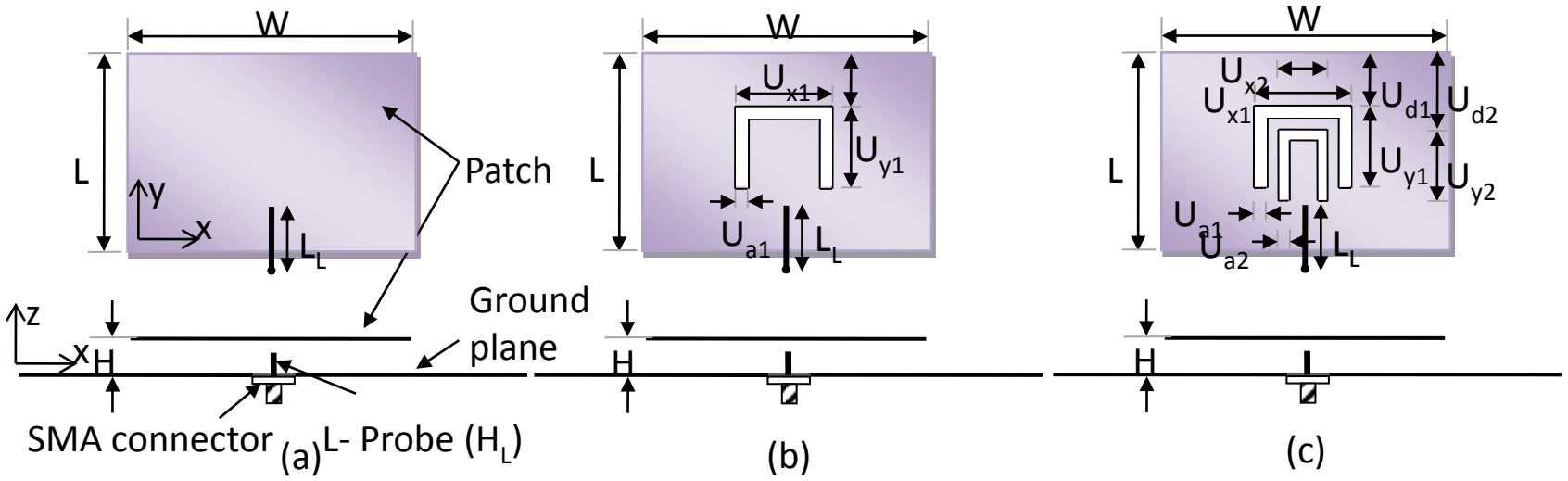

Fig.3.15 Geometry of the proposed antennas: (a) broadband, (b) dual band and (c) triple band.

Antenna	W	L	H	H_L	L_L	U_{a1}	U_{d1}	U_{x1}	U_{y1}	U_{a2}	U_{d2}	U_{x2}	U_{y2}
a	22	18	5	3.5	8.5								
b	22	18	5	3.5	8.5	0.8	2	7.5	10.8				
c	22	18	5	3.5	8.5	0.8	2	7.5	10.8	0.8	3.5	4.5	10.8

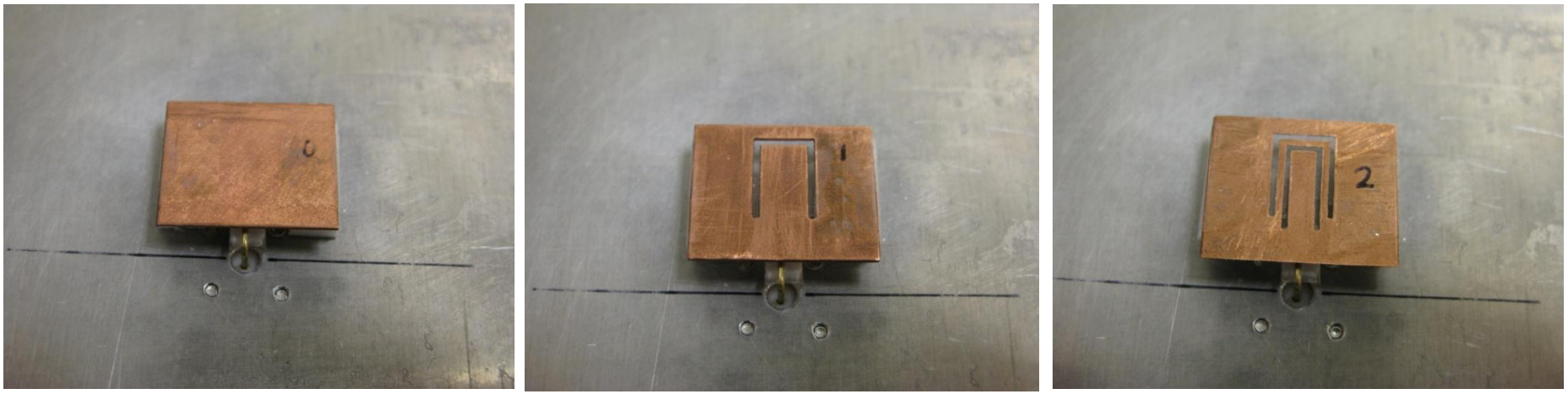

(a) (b) (c)

Fig. 3.16 Photos of the antenna prototypes: (a) broadband, (b) dual band and (c) triple band.

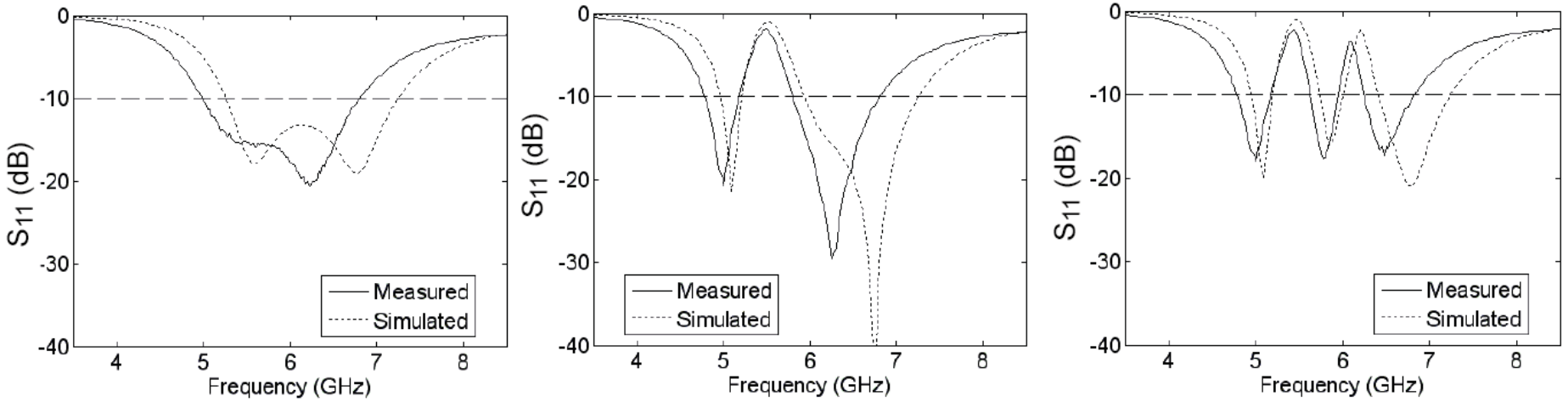

Fig. 3.17 Simulated and measured reflection coefficient of the proposed antennas: (a) broadband, (b) dual band and (c) triple band.

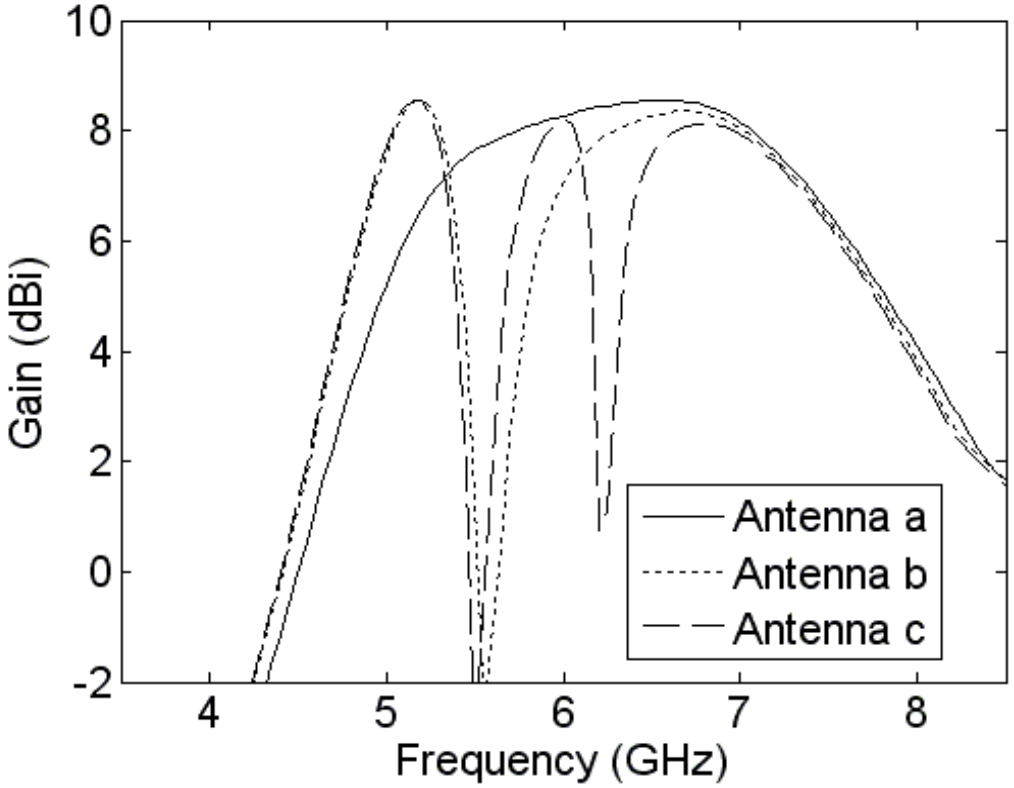
10
8
6
4
2
0
-2
Gain (dBi)
4
5
6
7
8
Frequency (GHz)
Antenna a
Antenna b
Antenna c

Table 3.3 Simulated and measured impedance bandwidths

Antenna	Simulation /GHz	Measurement /GHz
a	5.26-7.25 (31.8%)	5.00-6.80 (30.5%)
b	4.97-5.22 (4.9%), 5.94-7.26 (20%)	4.80-5.18 (7.6%), 5.80 -6.80(15.9%)
c	4.95-5.20 (4.9%), 5.74-6.00 (4.4%), 6.41-7.24 (12.2%)	4.80-5.18 (7.6%), 5.63-5.95 (5.5%), 6.25-6.83 (8.9%)

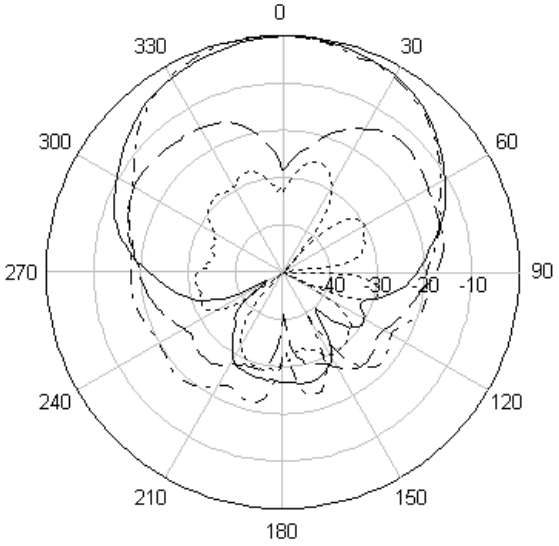

Antenna a @ 5.9 GHz

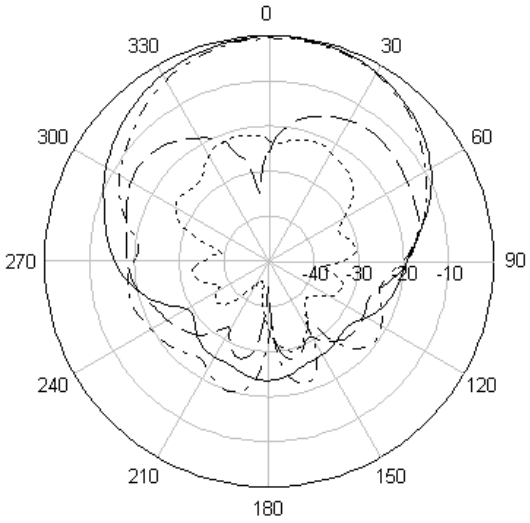

Antenna b @ 5.0 GHz

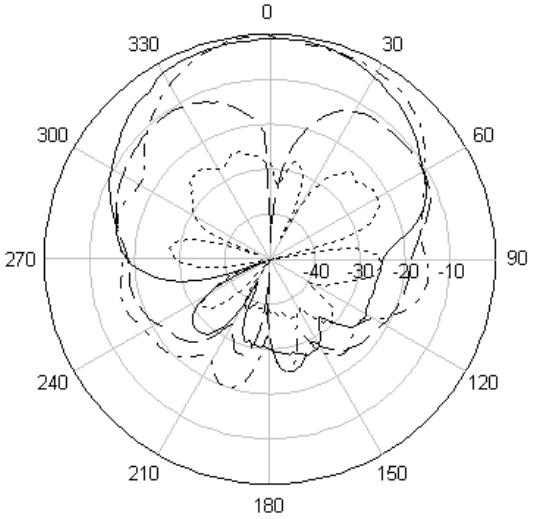

Antenna b @ 6.3 GHz

Fig. 3.18(a) Measured radiation patterns of the broadband antenna a of Table 3.3 at 5.9 GHz and dual band antenna b at 5.0 and 6.3 GHz.

(_____ H-Co, ___ ___ H-x, __.__ E-Co, …….. E-x)

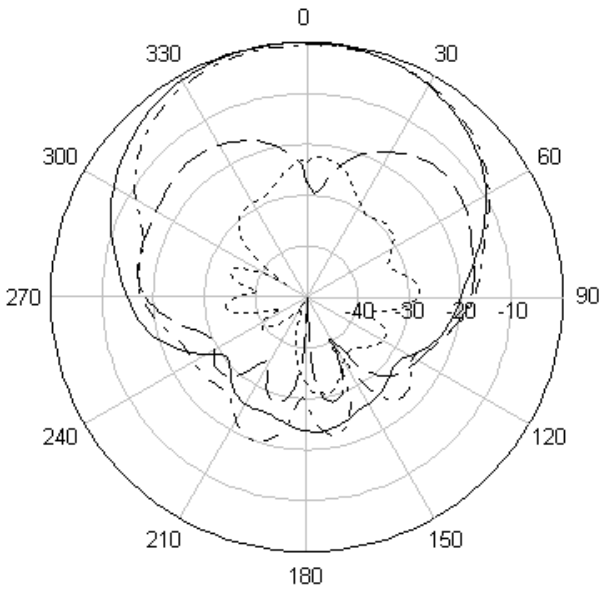

(a)

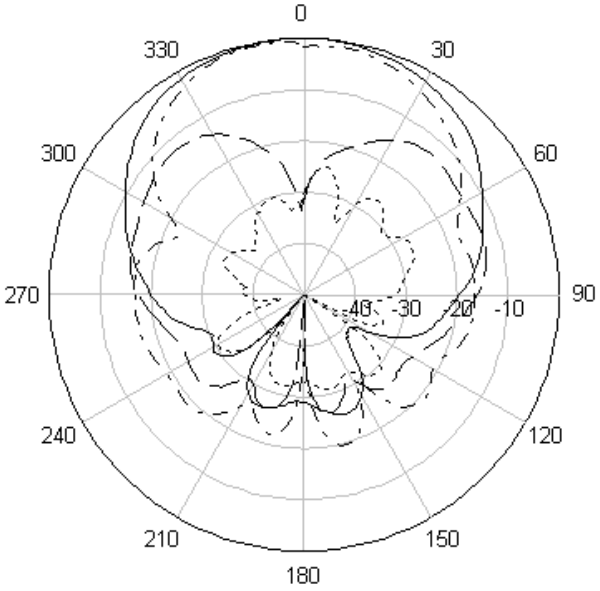

(b)

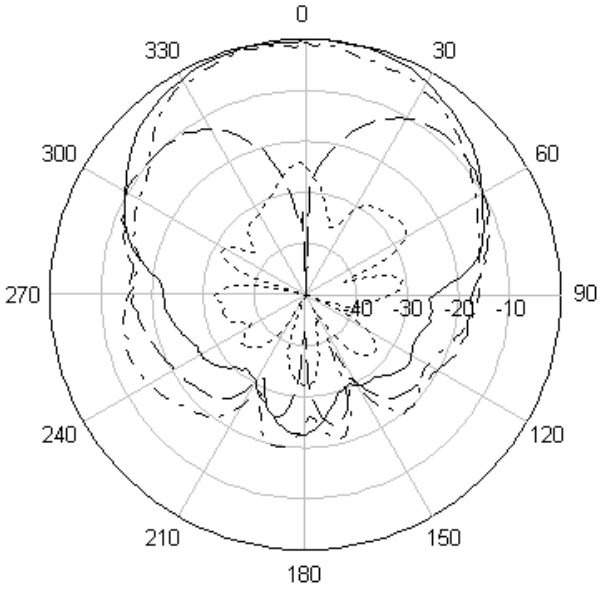

(c)

Fig. 3.18(b) Measured radiation patterns of the triple band antenna in Table 3.3 (Antenna c): (a) 5.0 GHz, (b) 5.8 GHz and (c) 6.55 GHz

(_____ H-Co, ___ ___ H-x, __.__ E-Co, …….. E-x)

7.4.3.2 Starting with the U-Slot Broadband Patch

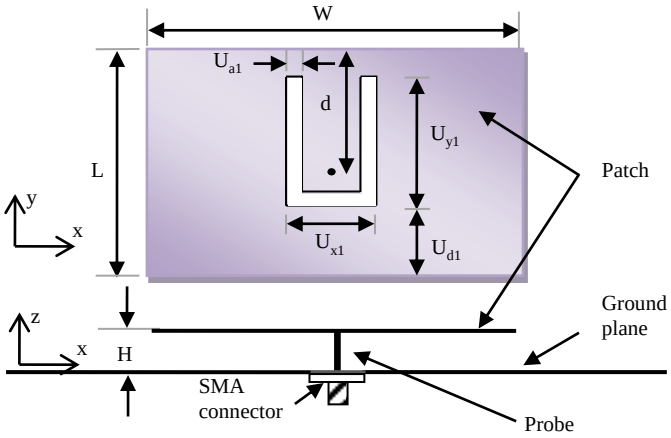

(a) Geometry of the broadband U-slot patch antenna

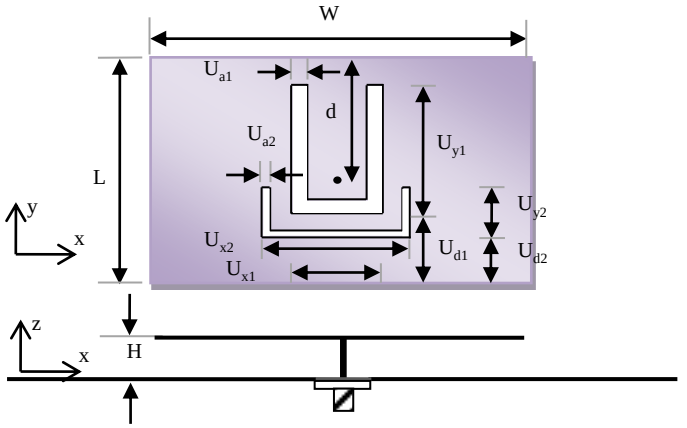

(b) Geometry of the dual-band patch antenna

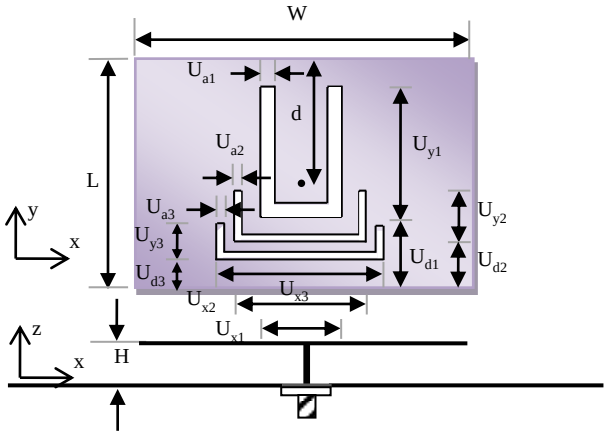

(c) Geometry of the triple-band patch antenna

Fig. 3.19 (a) Geometries of the single-layer single-patch dual and triple band patch antenna

Table 3.4 Dimensions of the proposed antennas (Unit: mm)
Ground Plane SIZE: 71 MM x 52 MM
THICKNESS OF PATCH METAL; 1 MM

Antenna	W	L	H	d	U_{a1}	U_{d1}	U_{x1}	U_{y1}
1a	35.5	26	6	13.5	2.1	4.8	12	19.5
1b	35.5	26	6	13.5	2.1	5.8	13	18.5
1c	35.5	26	6	14.5	2	5.8	14	18.7

Antenna	U_{a2}	U_{d2}	U_{x2}	U_{y2}	U_{a3}	U_{d3}	U_{x3}	U_{y3}
1a	-	-	-	-	-	-	-	-
1b	1	1.5	22	7	-	-	-	-
1c	1	3.5	18	9	1	1.5	22	4

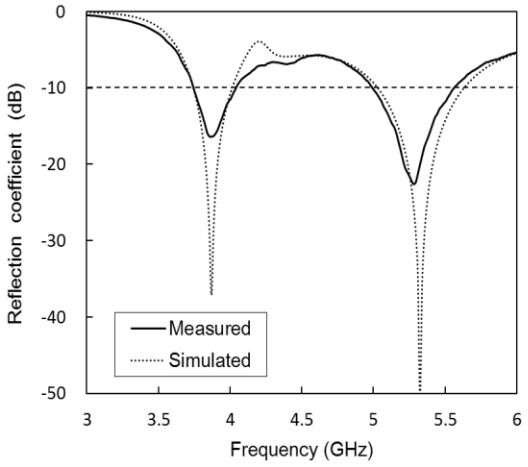

(i) Antenna 1(b)

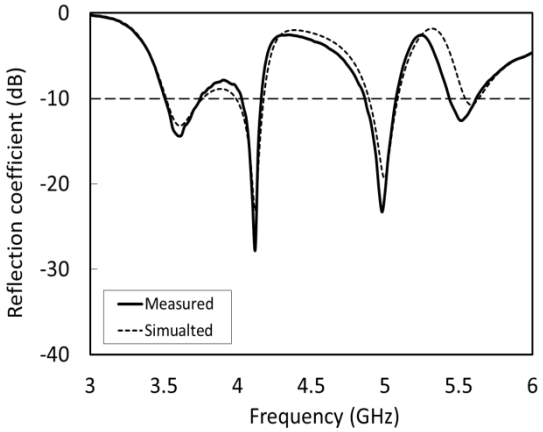

(ii) Antenna 1(c)

Fig. 3.20 Measured and simulated reflection coefficients of Antenna 1(b) and Antenna 1(c)

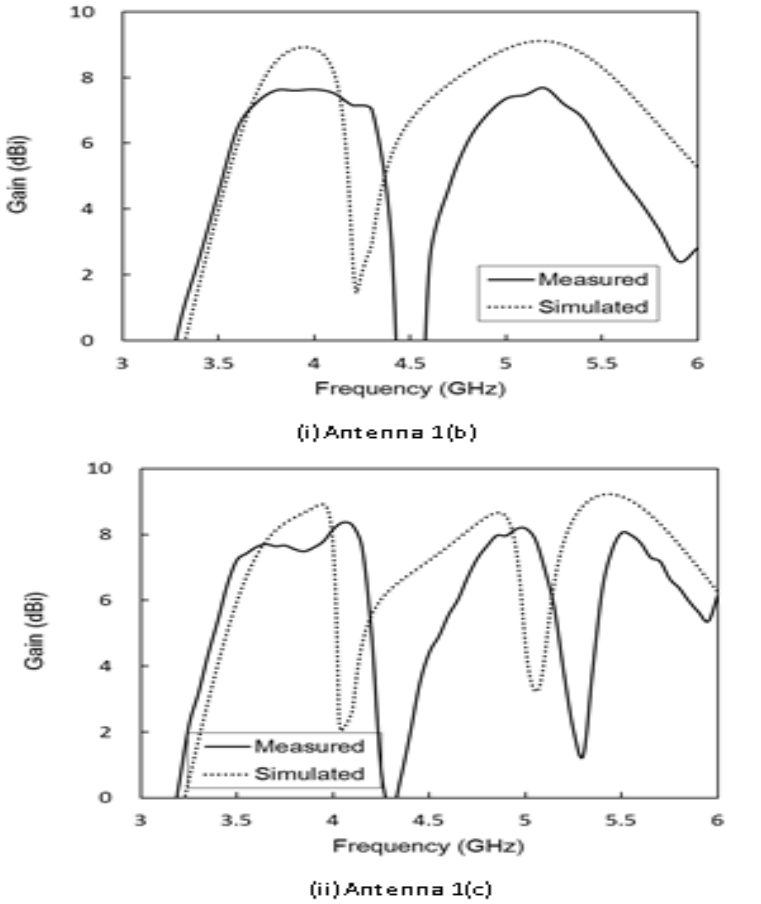

Fig. 9 Measured and simulated gains of antennas 1(b) and 1(c)

Fig. 3.21 Measured and simulated gains of antenna 1(b) and 1(c)

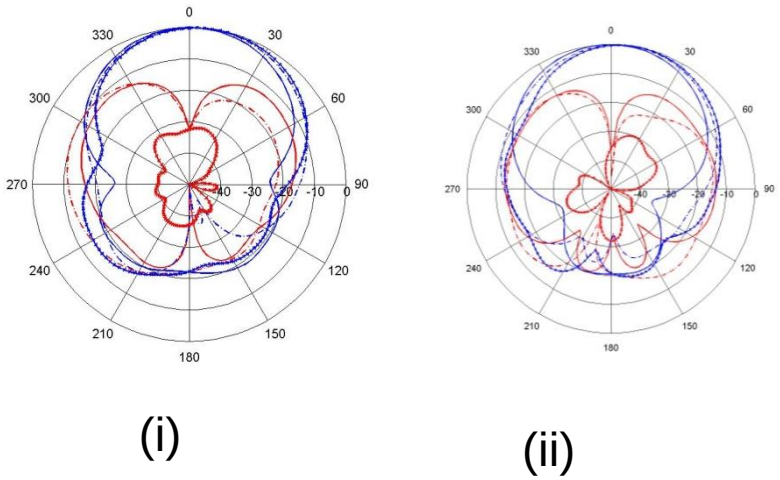

Fig.3.22 Measured radiation patterns of antenna 1(b): (i) 3.8 GHz and (ii) 5.2 GHz. (H: Φ = 0 º____ , Φ = 45 º __ .___ , Φ = 90 º- - - - , Co-pol - blue lines and X-pol –red lines)

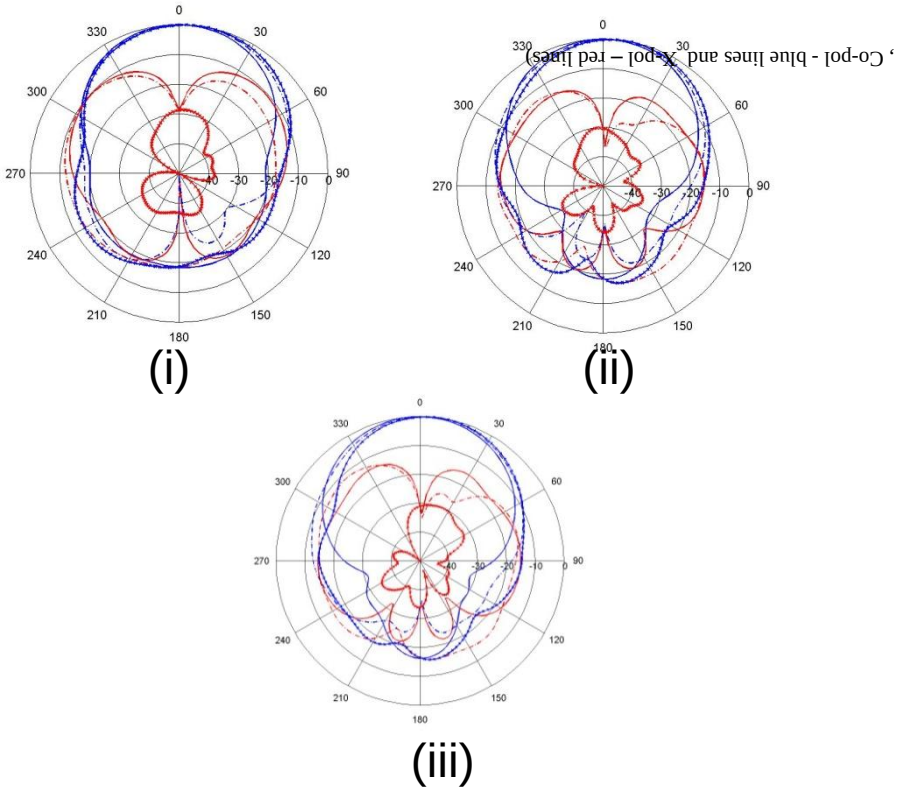

Fig. 3.23 Measured radiation patterns of antenna 1(c): (i) 3.7 GHz, (ii) 4.95 GHz and (iii) 5.55 GHz . (Φ = 0 º ___ , Φ = 45 º __ .___ , Φ = 90 º- - - - , Co-pol - blue lines and X-pol –red lines)

Concluding Remarks on section 7.4.3

- As mentioned previously, the method of designing dual/triple band antennas by cutting U-slots in the patches of a broadband patch antenna can also be applied to the M-probe fed patch and coaxial fed and aperture coupled stacked patches. A comprehensive account is reported in (Lee et al., 2013).

- Because the frequency bands are within the bandwidth of the antenna without slots, this method works when the frequency ratios are small, usually less than 1.5.

References for using U-slots in dual/triple band designs

K. F. Lee, K. M. Luk, K. F. Tong, S. M. Shum, T. Huynh and R. Q. Lee, "Experimental and simulation studies of the coaxially-fed U-slot rectangular patch antenna," IEE Proc.-Microw. Antennas, Propaga., Vol. 144, No. 5, pp. 354-358, 1997.

K. F. Lee, S.L.S. Yang, and A. Kishk, "Dual- and multi-band U-slot patch antennas," IEEE Antennas and Wireless Communication Letters, Vol. 7, pp. 645-648, 2008.

K. F. Lee, K. M. Luk , K. M. Mak, and S. L. S. Yang, "On the use of U-slots in the design of dual-and triple-band patch antennas," IEEE Antennas and Propag. Magazine, Vol. 53, pp. 60-74, June 2011.

W. C. Mok, S. H. Wong, K. M. Luk and K. F. Lee, "Single-layer single-patch dual-band and triple-band patch antennas," IEEE Transactions on Antennas and Propag., Vol. 61, No. 8, pp. 441-4344, 2013.

Prof. A. Kishk

Steven Yang

Ricky Chair

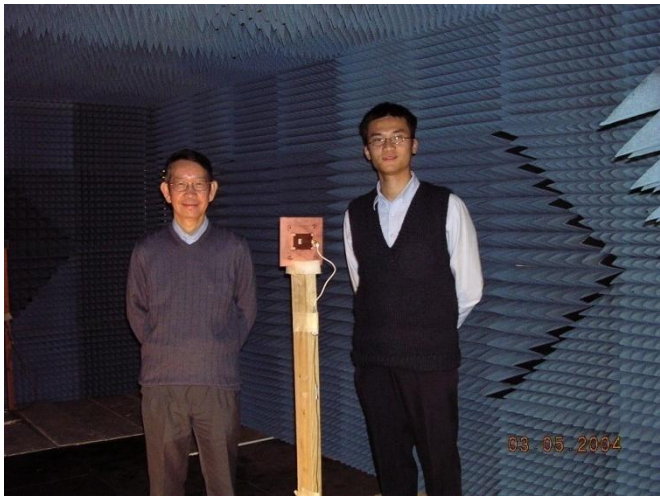

8. Design for Circular Polarization

8.1. Introductory remarks and general principles of single feed circularly polarized patch antennas
8.2. Square patch with truncated corners
  8.2.1. Effect of substrate thickness
  8.2.2. Addition of symmetric U-slot
8.3. Asymmetric U-slot CP patch antenna
8.4. Modified E-shaped CP patch antenna

8.1. Introductory remarks and general principles of single feed circularly polarized patch antenna

8.1.1 Axial ratio, axial ratio bandwidth, cross polarization

$\vec{E} = \left(A\hat{u}_1 + B\hat{u}_2 \right) E_o$ Linear Polarization; A and B positive real numbers

$\vec{E} = \left(A\hat{u}_1 \pm jB\hat{u}_2 \right) E_o$ Right elliptical +
Left elliptical -

A = B $\Leftrightarrow$ circular

- Axial ratio AR = B/A
- Axial ratio bandwidth (ARBW) – range of frequencies for which AR < 3 dB
- Cross polarization level : $|E_L|/|E_R|$ if E_R is copolarization

$|E_R|/|E_L|$ if E_L is copolarization

8.1.2. Applications of circularly polarization

a. When it is not possible to ascertain the polarization of an incoming wave due to multi-path propagation and/or reflection, it is more reliable to use circular polarization.

b. In operating radar in raining weather, circular polarization is found to minimize the clutter echoes received from raindrops, in relation to larger targets such as an aircraft.

c. In communication with satellites and space vehicles which are located above the earth's ionosphere, circular polarization is preferred over linear polarization. Examples: Direct Broadcasting Satellite (DBS) TV, Military Satellites and Global Navigation Satellite System.

GNSS Systems (from J. H. Wang, "Antennas for Global Navigation Satellite System", PIEEE, Vol. 100, No. 7, pp. 2350, 2012)

Table 1 Signals and Constellations of Major GNSS Systems: GPS, GLONASS, Galileo, and Compass

System	Country	Constellation	Coding	Carrier/Center Frequency (MHz)	Maximum Bandwidth (MHz)
GPS	USA	24 MEO (32 satellites in orbit in 2011 and under modernization)	CDMA	L1/ L1C: 1575.420 L2/ L2C: 1227.600 L5: 1176.45	30.69
GLONASS	Russia	24 MEO (24 satellites in orbit in 2011 and 6 active spares to be added)	FDMA CDMA FDMA CDMA CDMA CDMA	L1: 1602.000+k×0.5625* L1: 1575.420 L2: 1246.000+k×0.4375* L2: 1242.000 L3: 1202.025 L5: 1176.450	40.96
Galileo	European Union	27 MEO plus 3 spares (2 in operation in 2011)	CDMA	E1: 1575.420 E6: 1278.750 E5b: 1207.140 E5: 1191.795 E5a: 1176.450	40.96
Compass	China	27 MEO plus 5 GEO and 3 IGSO (4 MEO, 5 GEO, 5 IGSO in 2011)	CDMA	B1: 1559.052~1591.788 B2: 1162.220~1217.370 B3: 1250.618~1286.423	30.69

*k=0 to 24; each satellite having an FDMA channel.

Two conventional CP antennas

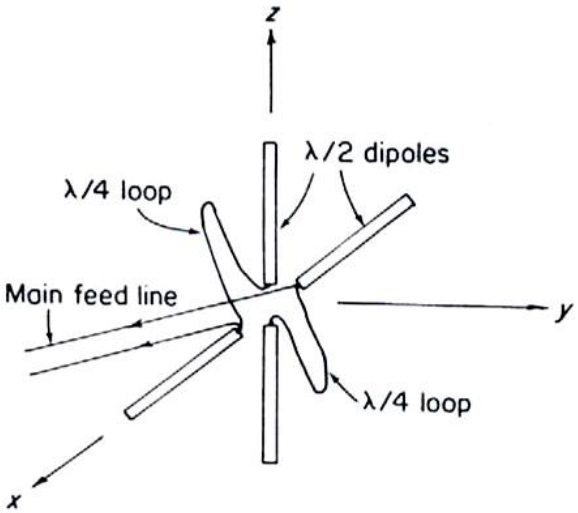

Cross dipole antenna

Yagi-Uda antenna of cross diploes

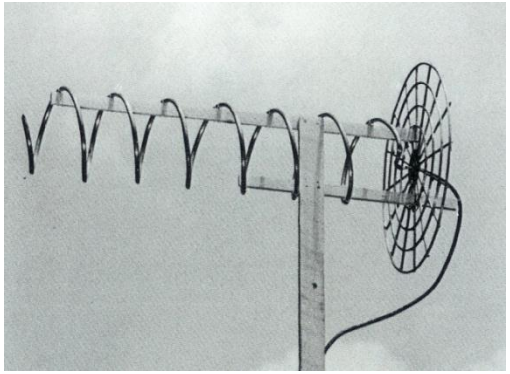

Helical antenna

Small Circularly Polarized Patch Antennas for CAPS (Chinese Area Positioning Systems)

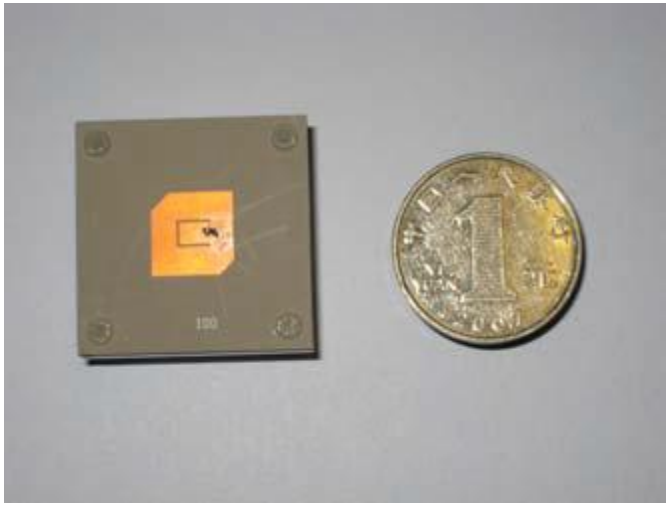

Freq: 3.88GHz
Patch Size: 11mm
GND Size: 30mm
Thickness: 3.18mm
dielectric constant: 10.2
Polarization: RHCP

8.1.3. Overview of circularly polarized patch antennas

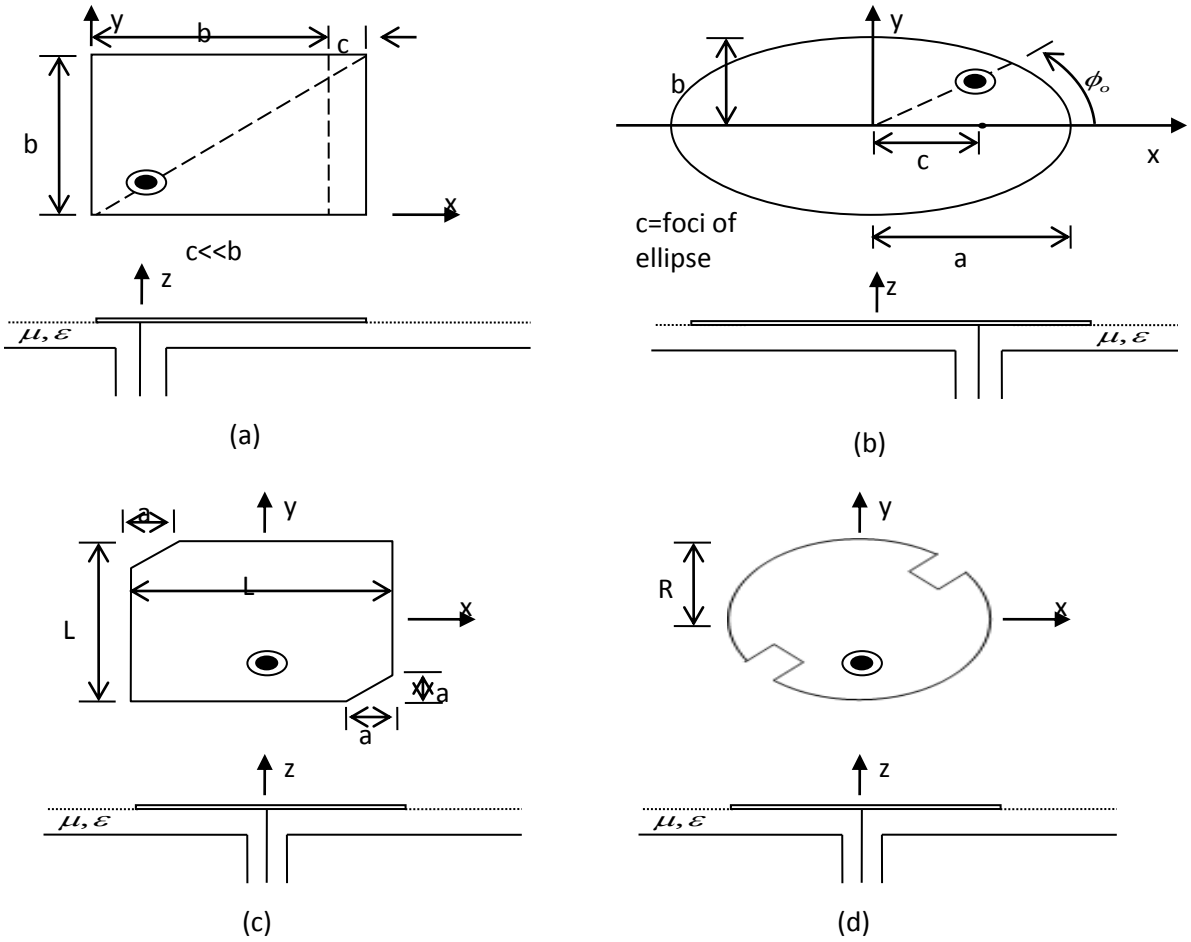

Fig.3.24 Single feed circularly polarized patches. (a) Almost square patch. (b) Almost circular (elliptical patch). (c) Square patch with truncated corners. (d) Circular patch with indentations.

Single feed CP patches shown above have very narrow bandwidth, typically 1% or less.

Dual Feed CP Patch Antenna

Each feed excites a linearly polarized mode.

- The two modes are of orthogonal polarization.
- A feeding network is to provide the two ports with equal amplitude but phase quadrature excitations.
- Achievable bandwidth much larger than single feed (~ 10%)
- Requires complicated feed network

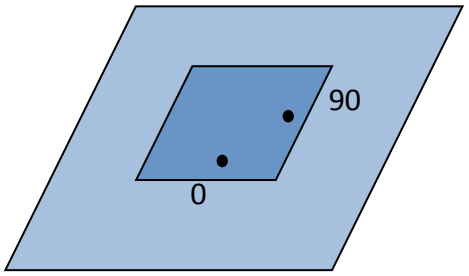

Fig.3.25 Dual feed CP patch antenna

The dual- orthogonal feeds excite two orthogonal modes with equal amplitude but in phase-quadrature. Several power divider circuit that have been successfully employed for CP generation are shown below.

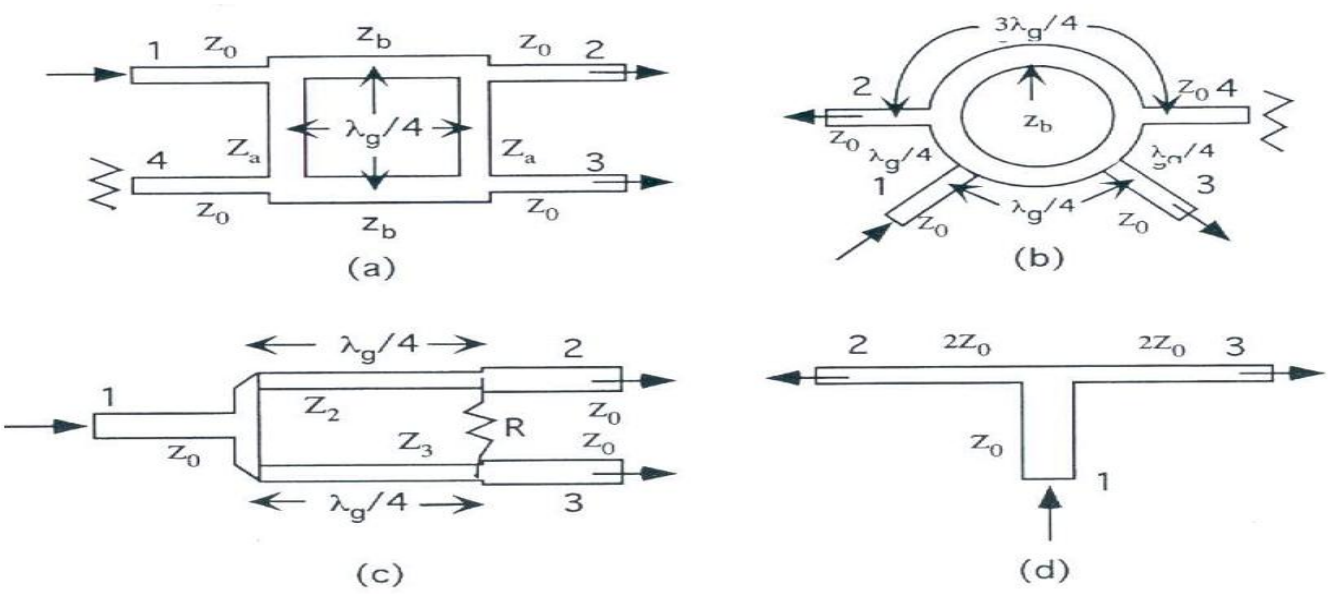

Fig. 3.26 Schematic diagrams of power dividers: (a) quadrature hybrid, (b) ring hybrid, (c) Wilkinson power divider, and (d) T-junction power divider

General Principles of Single feed circularly polarized patch antennas

a. The basic principle is that a perturbation of the dimensions be introduced such that, by feeding the patch at the appropriate location, two modes with orthogonal polarizations are generated with resonant frequencies which are slightly different.

b. In the almost square patch and the almost circular patch, the perturbation is in the form of one of the dimensions being slightly different from the other.

c. In the square patch with truncated corners and the circular patch with indentations, the perturbation is in the form of two slightly different diagonal lengths.

d. In the broadside direction, the amplitudes and phases of the radiated electric fields of the two orthogonal modes generated are illustrated in Fig. 16.4. The resonant frequency of these modes are f_a and f_b respectively.

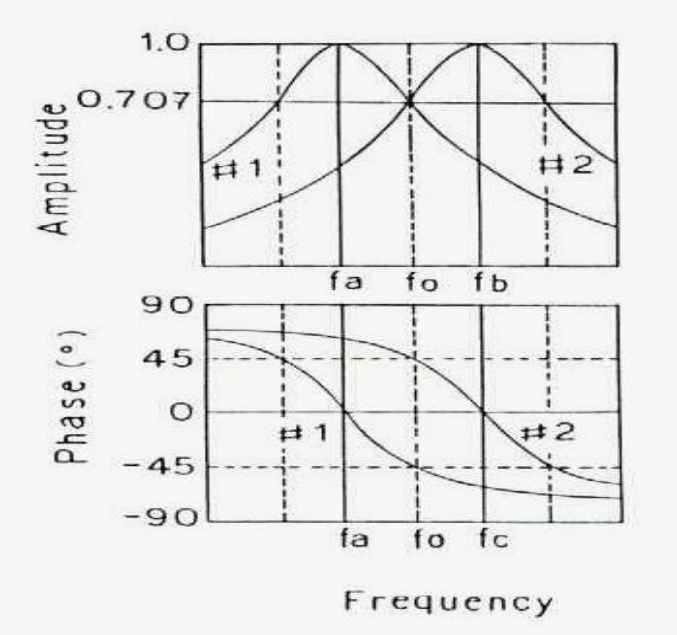

Fig. 3.27 The amplitude and phase of two orthogonal modes

e. At the frequency f_o, approximately mid-way between f_a and f_b, the amplitudes of the two modes are equal and the phases differ by 90^o, resulting in circular polarization.

f. This condition for perfect CP occurs only at f_o and in the broadside direction. As the frequency deviates from f_o and/or the direction is off broadside, elliptical polarization results.

g. The axial ratio bandwidth (ARBW) is defined as the range of frequencies for which the axial ratio is less than 3 dB. The usable bandwidth of the antenna is the range of frequencies for which both AR < 3 dB and VSWR < 2.

h. The advantage of using single feed design to obtain CP is its simplicity. However, the antenna bandwidth is very narrow, typically less than 1%.

i. We shall show that the bandwidth of single feed CP antennas can be increased several fold by cutting a U-slot in the patch.

8.2 Square Patch with Truncated Corners

8.2.1 Effect of Substrate Thickness

• Consider the square patch with truncated corners shown in Fig. 3.28. Substrate is air.

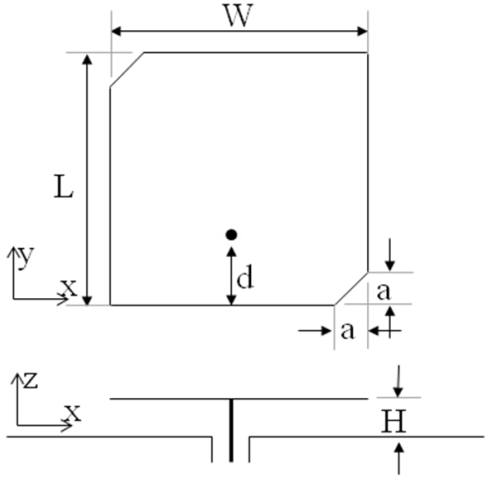

Fig. 3.28 Geometry of single probe feed square patch with truncated corners

Table 3.5 Parameters of antenna as shown in Fig. 4. W=L=28.6 mm

Case	Substrate thickness (H)		a	d
1	1 mm	$0.016\lambda_o$	3.3	8.2
2	1.5 mm	$0.024\lambda_o$	4.5	7.2
3	2 mm	$0.032\lambda_o$	4.9	5.5
4	3 mm	$0.046\lambda_o$	5.9	5.1
5	4 mm	$0.06\lambda_o$	6.9	4.3

Table 3.6 Simulation RLBW and ARBW for the antennas shown in Table 1

Case	Substrate thickness (H)		Simulation (GHz)	
			RL BW	AR BW
1	1 mm	$0.016\lambda_o$	4.86-5.06 (4.0%)	4.90-4.94 (0.82%)
2	1.5 mm	$0.024\lambda_o$	4.88-5.08 (4.0%)	4.79-4.86 (1.45%)
3	2 mm	$0.032\lambda_o$	4.85-5.11 (5.2%)	4.68-4.78 (2.1%)
4	3 mm	$0.046\lambda_o$	4.81-5.18 (7.4%)	4.52-4.66 (3.1%)
5	4 mm	$0.06\lambda_o$	4.89-5.09 (4.0%)	4.40-4.57 (3.8%)

- It is seen that, as the substrate thickness increases from 1 mm ($0.016\lambda_o$) to 3 mm ($0.046\lambda_o$), the RL bandwidth increases from 4.0% to 7.4% while the AR bandwidth increases from 0.82% to 3.1%.
- When the thickness increases further to 4 mm ($0.06\lambda_o$), the RL BW drops to 4.0% while the AR BW continues to increase to 3.8%.
- The important point to note is that, beginning with case 2, the two frequency bands do not overlap. Thus, only in case 1 are the AR BW lies within the RL BW, and the useful frequency band is determined by the AR bandwidth, from 4.90 to 4.94 GHz, corresponding to 0.82%.

8.2.2 Broadbanding using symmetric U-slot

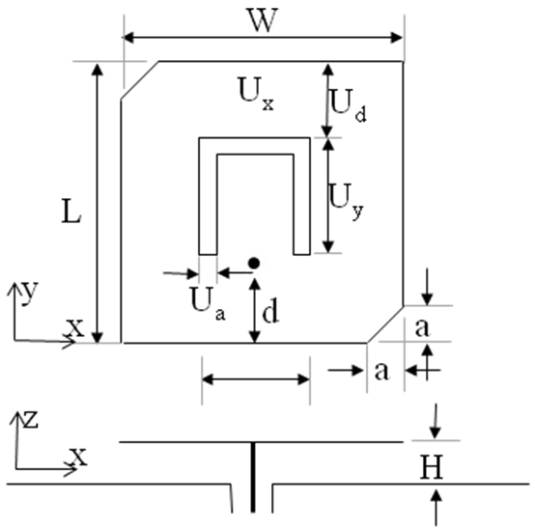

Fig. 3.29 Geometry of the single feed U-slot perturbed patch antenna. Air substrate. W=L=28.6 mm.

Table 3.6 Parameters of the antenna as shown in Fig. 3.29

Case	Substrate thickness (H)		a	d	U_a	U_d	U_x	U_y
6	4 mm	$0.05\lambda_o$	5.7	12.6	1	9.8	12	14
7	6 mm	$0.08\lambda_o$	7.7	9.6	1	9.8	12	14
8	7.5 mm	$0.1\lambda_o$	8.2	5.6	1	9.8	11	14

8.2.2 Broadbanding using symmetric U-slot

Table 3.7 Results of the different cases as shown in Table 3

Case	Substrate thickness (H)		Simulation (GHz)		Measurement (GHz)	
			RL BW	AR BW	RL BW	AR BW
6	4 mm	$0.05\lambda_o$	3.83-4.18 (8.7%)	3.96-4.05 (2.2%)	-	-
7	6 mm	$0.08\lambda_o$	3.73-4.2 (11.9%)	3.96-4.12 (4.0%)	3.66-4.16 (12.8%)	3.91-4.12 (5.23%)
8	7.5 mm	$0.1\lambda_o$	3.84-4.08 (6.1%)	3.84-4.09 (6.3%)	3.88-4.08 (5.0%)	3.82-4.05 (5.84%)

8.2.2 Broadbanding using Symmetric U-slot

The following is observed:

1. When the U-slot is added on the patch, the resonant frequency is lowered compared to the case without the U-slot.

2. By adjusting the dimensions of the U-slot, the RL and AR bandwidths can be tuned to overlap.

3. The measured overlapping bandwidth is 5.23% for H= 6 mm (0.08 λ_o) and 5.84% for H= 7.5 mm (0.1 λ_o). This is to be compared to 0.82% achievable for the case of no U-slot. This is achieved, of course, at the expense of significantly increasing the thickness of the antenna.

- The simulation and measurements results for return loss, axial ratio, and radiation patterns at one frequency for the cases of H=6 mm and H=7.5 mm are shown in Figs. 3.30 and 3.31.

8.2.2 Broadbanding using Symmetric U-slot

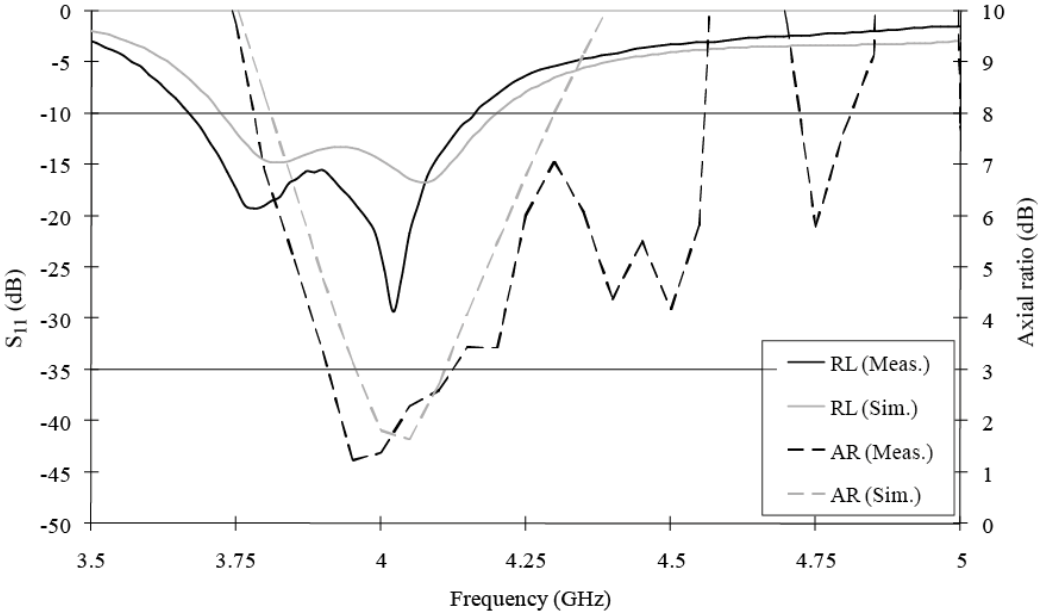

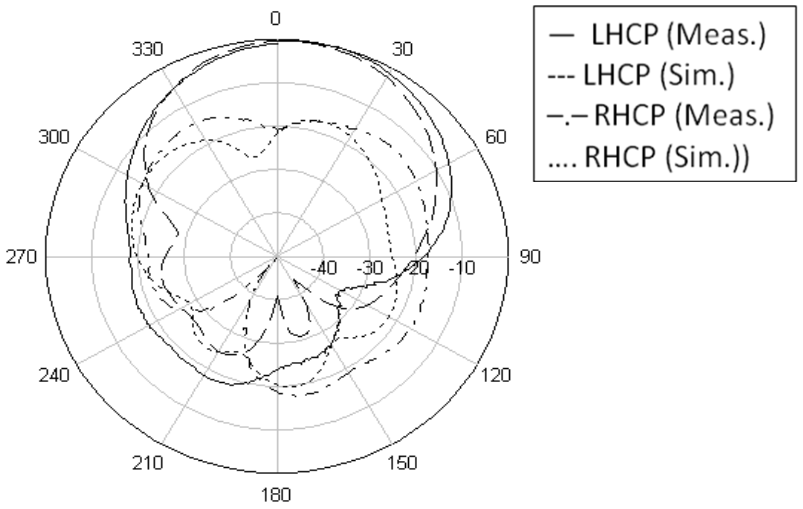

Fig. 3.30 Simulated and measured performance of case 7, radiation patterns are at 3.95GHz.

8.2.2 Broadbanding using symmetric U-slot

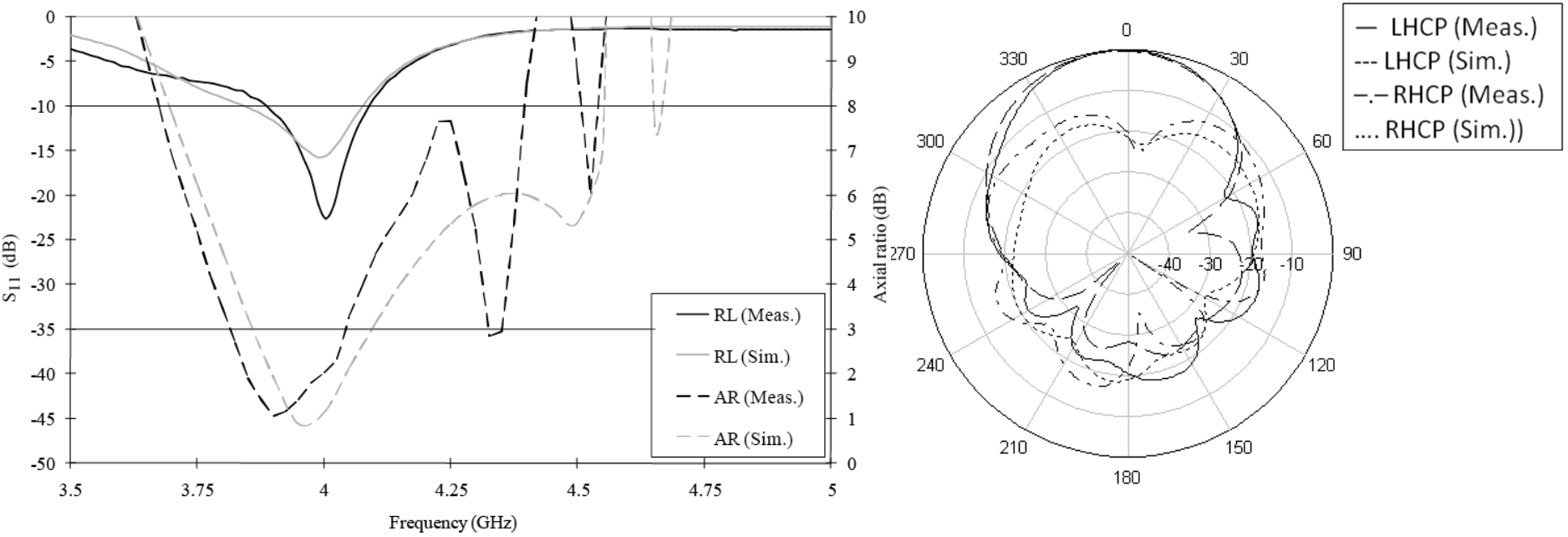

Fig. 3.31 Simulated and measured performance of case 8, radiation patterns are at 4GHz.

8.2.3 Truncated-Corner Square Patch with Symmetric U-slot – Comparison of Air and Material Substrates

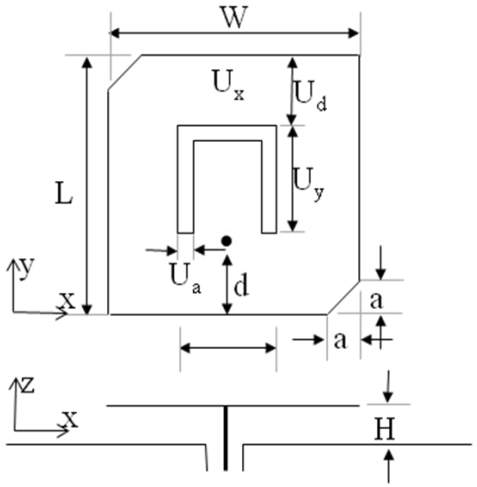

Table 3.8 Antenna Parameters

ε_r	Substrate thickness (H)		W	L	a	d	U_a	U_d	U_x	U_y
1	8	$(0.066\lambda_o)$	51.4	51.4	12.2	12.6	1.8	28.6	23.4	11.7
1	10	$(0.082\lambda_o)$	50.5	50.5	12.9	9.7	1.8	26.1	23	17
2.2	5.4	$(0.07\lambda_g)$	34.6	34.6	7	8.5	1.2	19.3	15.7	7.9
2.2	6.7	$(0.089\lambda_g)$	34	34	7.7	6.5	1.2	17.6	15.5	11.5
4	4	$(0.073\lambda_g)$	25.3	25.3	4.1	4.8	0.9	10.1	9.5	3.5
4	5	$(0.091\lambda_g)$	25.3	25.3	4.5	4.8	0.9	12.1	11.5	3.5

Table 3.9 Simulation Results for RLBW, ARBW and Peak Gain

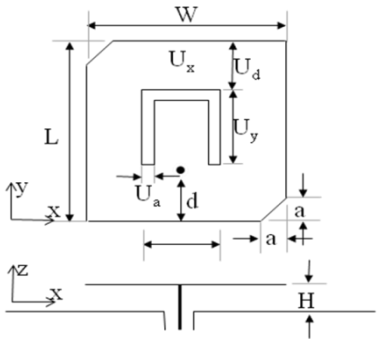

ε_r	H (mm)	RLBW (GHz)	ARBW (GHz)		Peak Gain (dBi)
		(IE3D)	(IE3D)	(HFSS)	
1	8 ($0.066\lambda_0$)	2.25-2.54 (12.1%)	2.35-2.44 (3.76%)	2.33-2.42(3.8%)	9.5
1	10 ($0.082\lambda_0$)	2.19-2.41 (9.57%)	2.28-2.38 (4.29%)	2.26-2.35 (3.91%)	9.0
2.2	5.4 ($0.07\lambda_g$)	2.5-2.78(10.6%)	2.57-2.64(2.69%)	2.55-2.61(2.33%)	6.5
2.2	6.7 ($0.089\lambda_g$)	2.48-2.85(13.9%)	2.52-2.61(3.51%)	2.5-2.59(3.54%)	6.2
4	4 ($0.073\lambda_g$)	2.67-2.80(4.75%)	2.70-2.75(1.83%)	2.69-2.73(1.48%)	5.1
4	5 ($0.091\lambda_g$)	2.6-2.83(8.47%)	2.64-2.70(2.25%)	2.62-2.67(1.89%)	4.7

Observations – Symmetric U-slot

- For each of the case shown, the ARBW lies within the RLBW so the BW of the antenna is determined by the ARBW.
- The ARBW decreases as ε_r increases. It increases slightly as the thickness increases from 8 mm to 10 mm.
- The results for ARBW from IE3D and HFSS are in good agreement.
- The peak gain for $\varepsilon_r = 1$ is about 9.5 dBi for H=8 mm and 9.0 dBi for H=10 mm.
- The corresponding values for ε_r =2.2 are 6.5 dBi and 6.2 dBi. For ε_r =4.0, they are 5.1 dBi and 4.7 dBi.

Animation

Electric Field Distribution Under the Patch

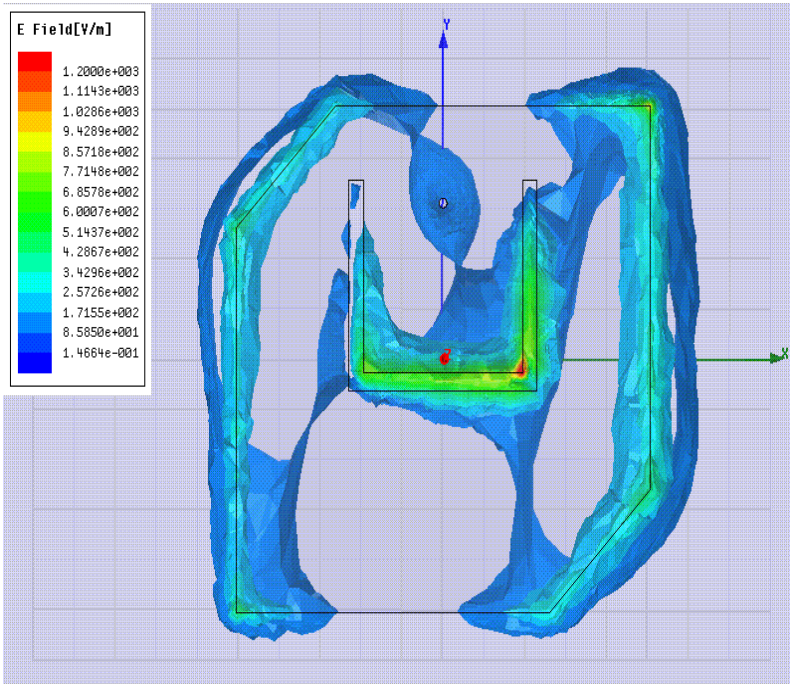

Electric field distribution in the air substrate

8.3 CP square patch antenna with asymmetric U-slot

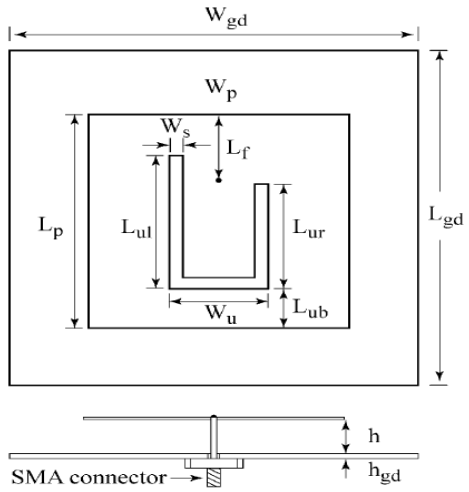

Fig. 3.32 Geometry of the single feed CP square patch antenna with asymeetric U-slot

In this design, first reported by Tong et al., CP is generated using an unequal arm U-slot. Corners of the square patch need not be truncated. In addition to generating CP, the slot increases the RLBW and enables the ARBW and RLBW to be tuned to overlap. Tong et al. obtained 3.9 % BW with center freq. 2.31 GHz was for air substrate of thickness $0.085\lambda_o$.

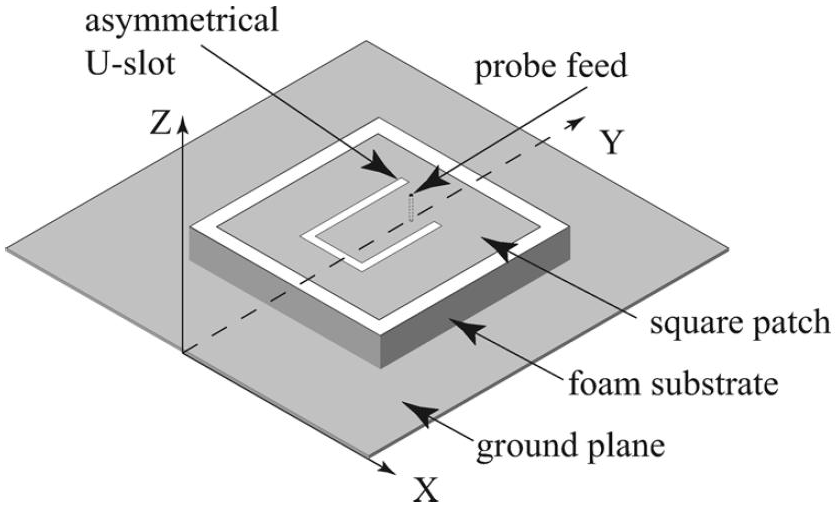

- K. F. Tong, T. P. Wong, “Circularly polarized U-slot antenna,” IEEE Trans. Antennas Propag., vol. 55 (8) pp.2382-2385, Aug. 2007.

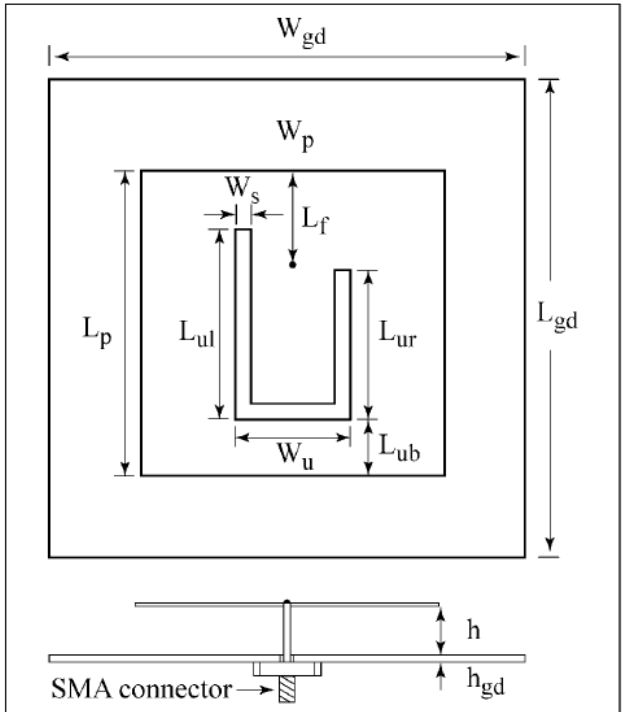

L_p	W_p	h	L_{ul}	L_{ur}	L_{ub}
44.7	44.7	11.0	27.8	21.8	8.3
W_u	W_s	L_f	L_{gd}	W_{gd}	h_{gd}
16.9	2.3	13.9	102	102	3

Asymmetrical U-slot on a Patch - Animation

Electric field in the air substrate

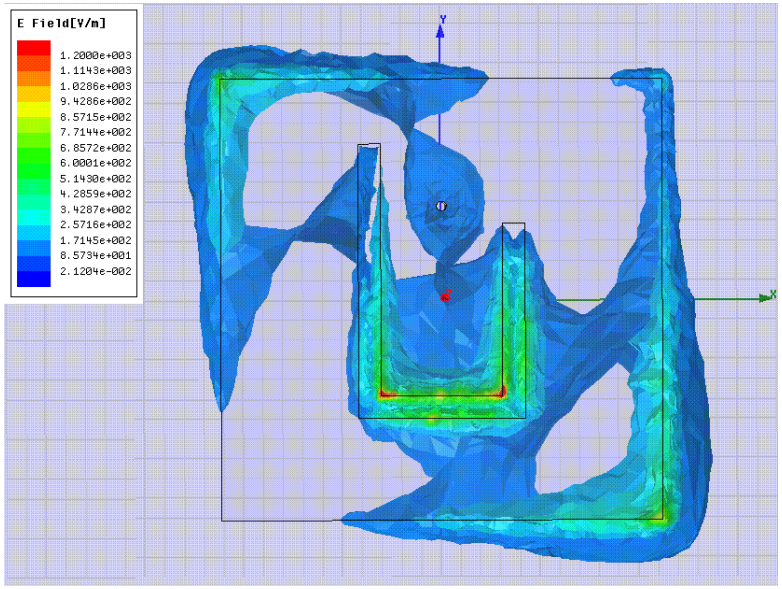

K-F. Tong, and T-P. Wong, “Circularly polarized U-slot antenna”, *IEEE Trans. Antennas Propag.*, vol. 55, no. 8, pp. 2382–2385, Aug. 2007.

Square patch with asymmetric U-Slot – Comparison of air and material substrate

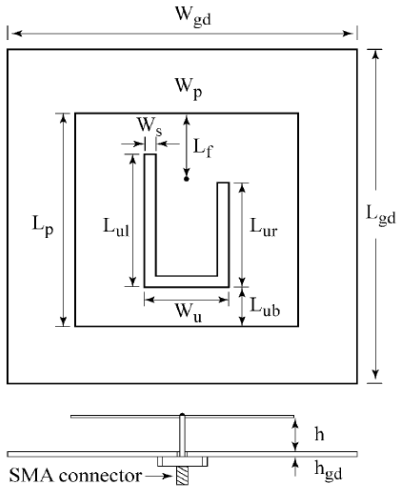

Table 3.10 Antenna Parameters

ε_r	H	L_p	W_p	L_{ul}	L_{ur}	L_{ub}	W_u	W_s	L_f
1	8 ($0.064\lambda_o$)	44.7	44.7	25.8	20.8	8.3	18.9	2.3	12.9
1	10($0.082\lambda_o$)	44.7	44.7	27.8	19.8	10.3	16.9	2.3	12.9
2.2	5.4 ($0.071\lambda_g$)	30.1	30.1	17.4	14.5	5.6	12.7	1.55	8.7
2.2	6.7($0.091\lambda_g$)	30.1	30.1	18.7	13.3	6.9	11.4	1.55	8.7
4	4 ($0.075\lambda_g$)	22.4	22.4	12.4	8.4	4.7	9.5	1.15	9.5
4	5 ($0.091\lambda_g$)	22.4	22.4	13.4	9.4	3.7	9.5	1.15	9.5

Table 3.11 Simulation Results for RLBW, ARBW and Peak Gain

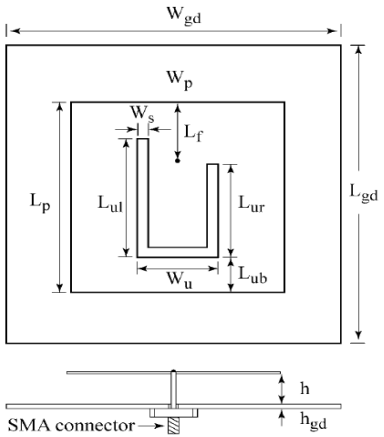

ε_r	H (mm)	RLBW (GHz)	ARBW (GHz)		Peak Gain (dBi)
		(IE3D)	(IE3D)	(HFSS)	
1	8 ($0.064\lambda_o$)	2.34-2.49 (6.21%)	2.4-2.47 (2.87%)	2.39--2.45(2.89%)	9.1
1	10 ($0.082\lambda_o$)	2.34-2.57 (9.37%)	2.35-2.45(4.17%)	2.34-2.44(3.98%)	8.75
2.2	5.4($0.071\lambda_g$)	2.61-2.70(3.39%)	2.62-2.67(1.89%)	2.61-2.67(2.08%)	6.2
2.2	6.7($0.091\ \lambda_g$)	2.57-2.89(11.7%)	2.58-2.66(3.05%)	2.57-2.65(3.06%)	6.1
4	4 ($0.075\ \lambda_g$)	2.74-2.86(4.29%)	2.80-2.84(1.42%)	2.79-2.83(1.43%)	4.9
4	5 ($0.091\ \lambda_g$)	2.63-2.85(8.03%)	2.72-2.77(1.82%)	2.71-2.78(1.83%)	4.8

Observations – Asymmetric Slot

- For each of the case shown, the ARBW lies within the RLBW so the BW of the antenna is determined by the ARBW.
- The ARBW decreases as ε_r increases. It increases slightly as the thickness increases from 8 mm to 10 mm.
- The results for ARBW from IE3D and HFSS are in good agreement.
- The peak gain for ε_r is about 9.1 dBi for H=8 mm and 8.75 dBi for H=10 mm.
- The corresponding values for ε_r =2.2 are 6.2 dBi and 6.1 dBi. For ε_r =4.0, they are 4.9 dBi and 4.8 dBi.

Concluding remarks

Studies of the two designs for CP utilizing U-slots etched on a square patch have been presented for both air and material substrates. Both designs are simple, and require only a single probe feed. In the first design, the truncated square patch generates circular polarization while the symmetric U-slot allows the use of thick substrates since it broadens the RLBW and tunes the ARBW to overlap with the RLBW. In the second design, the symmetric U-slot performs all the above functions. For the same thickness, both the bandwidth and the gain of the truncated square patch with symmetrical U-slot is slightly larger than the square patch with asymmetric slot.

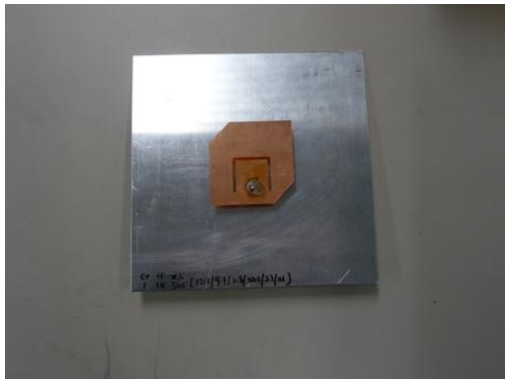

(a) Truncated-corner square patch with symmetric U-slot , air substrate

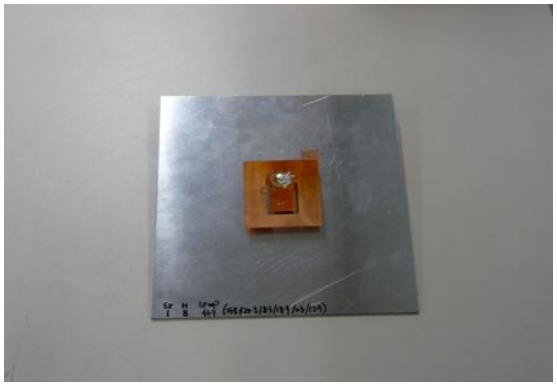

(b) Square patch with asymmetric U-slot, air substrate

Dual-band circularly polarized patch antenna using asymmetric U-Slots

A single feed stacked microstrip antenna with asymmetric U-slots covering two bands can be realized (Nayeri et al. 2013).

Similar or opposite polarizations for each band can be achieved by employing Similar or opposite symmetries in the U-slots of the lower and upper patches.

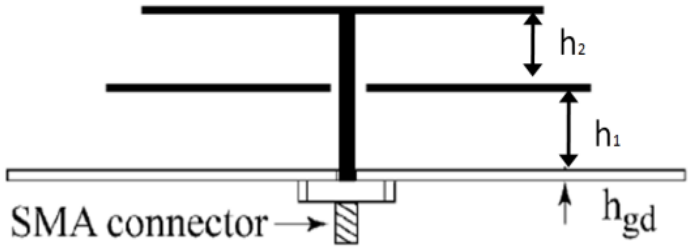

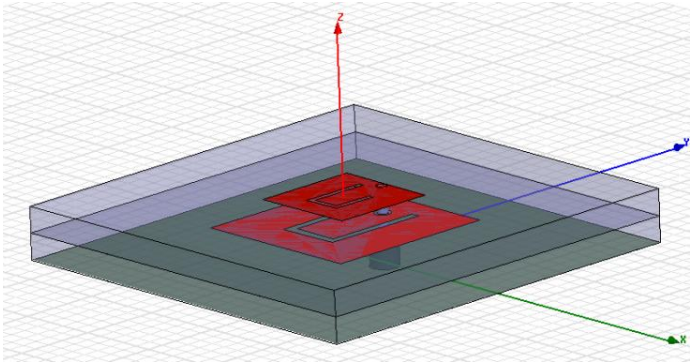

8.4 Circularly Polarized E-Shaped Patch Antenna

8.4.1 Introduction

THE U-SLOT PATCH AND THE E PATCH

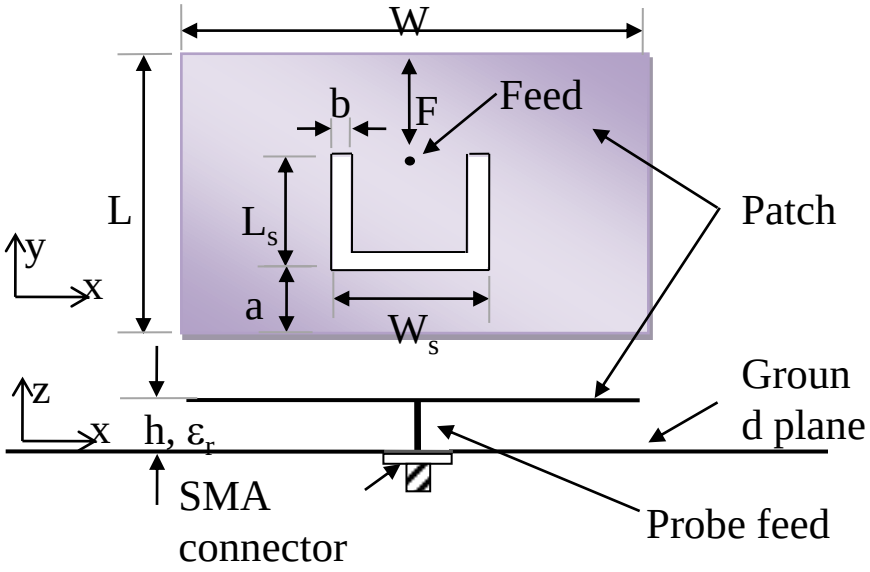

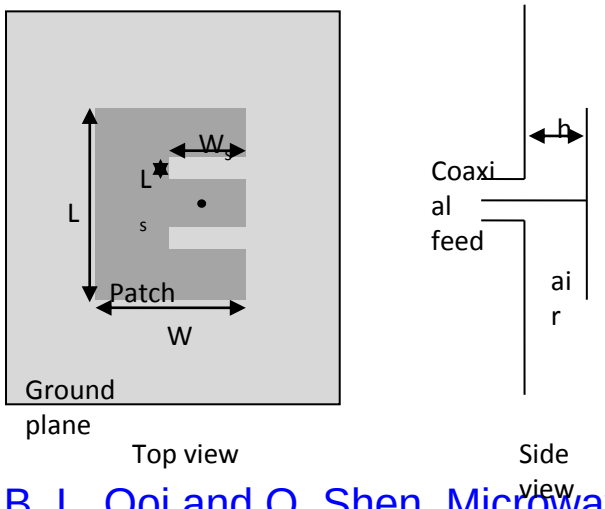

[1] T. Huynh and K. F. Lee, "Single-layer single-patch wideband microstrip antenna," *Electronics Letters*, Vol. 31, No. 16, pp. 1310-1312, 1995.

[2] B. L. Ooi and Q. Shen, Microwave and Optical Tech. Lett. , Vol. 27, pp. 348-352, 2000.
F. Yang, Z. Z. Zhang, Z. Ye and Y. Rami-Samii, IEEE Trans. Antennas and Propagat., Vo. 49, No. 7, pp. 1049-1100, 2001.

For the linearly polarized (LP) lowest mode, both patches achieve over 30% impedance bandwidth for air substrate thickness of about 0.08 λ

Square patch with asymmetric U-slot

K. F. Tong, T. P. Wong, IEEE AP Trans. Vol. 55, pp. 2382-2385, 20

BW (AR < 3 dB; RL < -10 dB) about 3.9 % for 0.085 λ_o thickness

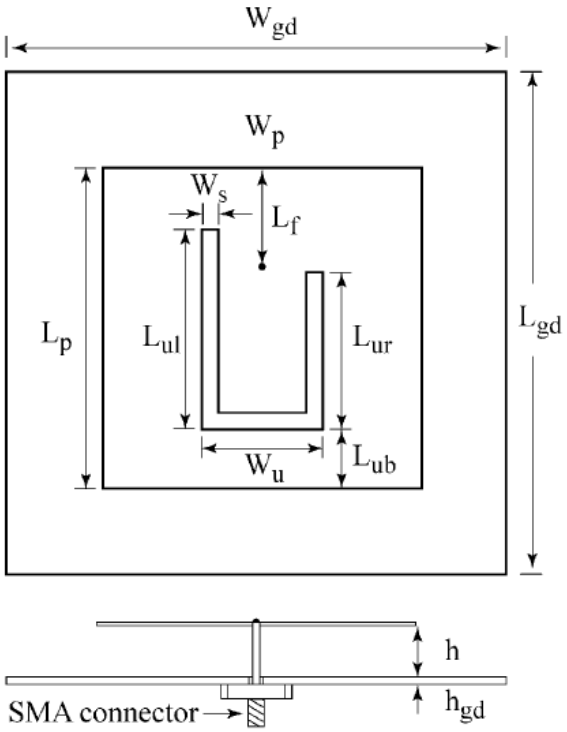

Question: Can patch with asymmetrical parallel slots (modified E-shaped) produce CP?

In 2010, student Ahmed Khidre, was assigned to investigate the E shaped patch along the following lines (as a project for the microstrip antenna course:

Idea:

- Making the two slots unequal ➔ introduce asymmetry ➔ two orthogonal current components on the patch
- Adjusting the ratio between two slots ➔ circularly polarized fields could be excited.

Goal: Designing single feed-single layer CP E patch antenna with wide band axial ratio (>5%) for 2.45GHz WLAN

8.4.2 Design procedure and prototype

1. Design LP wide band antenna at the desired band as in [Yang et al. 2001]
2. For LHCP, begin with making the length Ls2 shorter (while Ls1 is fixed) until a minimum axial-ratio level is obtained. The opposite procedure should be followed if RHCP is required.
3. Change the probe position F to improve the axial-ratio level, as well as aligning the S_{11} band with the axial-ratio band.
4. Adjust length of lower slot Ls1 to fine tune the axial-ratio level, as well as alignment with the S_{11} band.

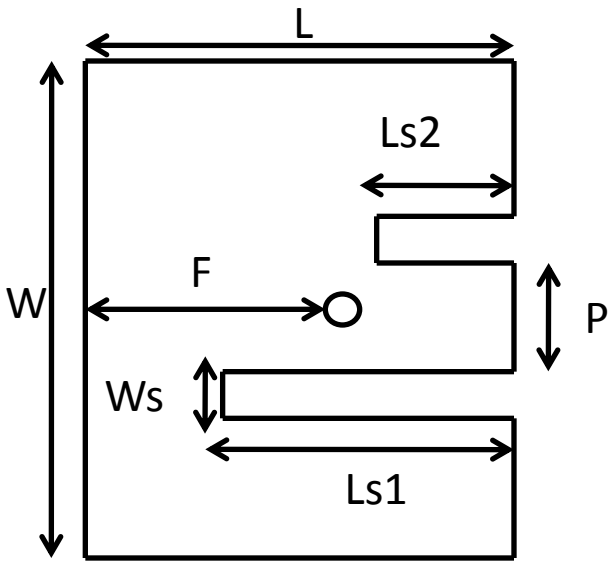

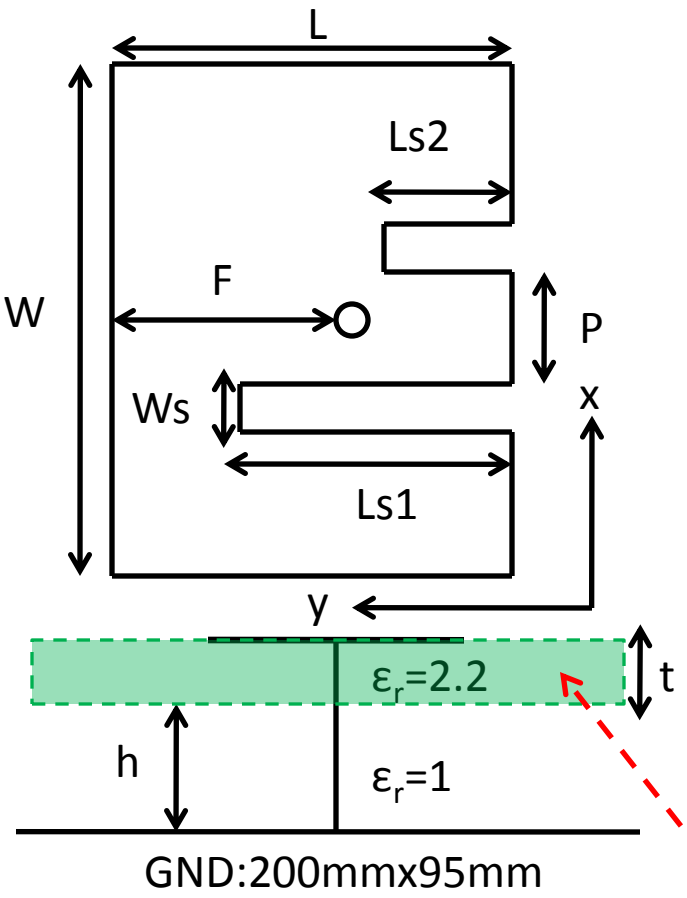

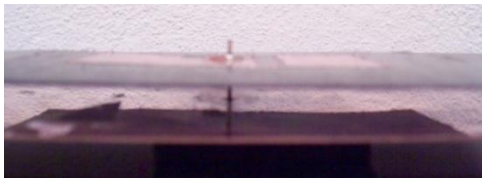

Thin copper clad substrate is used for milling the top patch which enable etching with higher accuracy of patch dimensions .

W	L	Ls1	Ls2	P	F	h	Ws	t
76mm	45mm	40mm	17mm	14mm	29mm	10mm	7mm	0.787mm

Fig. 3.33 Prototype E-shaped CP Antenna

Measurement results

Impedance bandwidth (S_{11} < -10 dB)	**2.34 – 2.57 GHz**	**9.37 %**
Axial ratio bandwidth (AR < 3 dB)	**2.30-2.64 GHz**	**13.9%**
Bandwidth (S_{11} < -10 dB; AR < 3 dB)	**2.34 – 2.57 GHz**	**9 %**

Maximum gain	**8.3 dB**	
3 dB Gain bandwidth	**2.27-2.65 GHz**	**14.6 %**

Field animation at 2.45 GHz

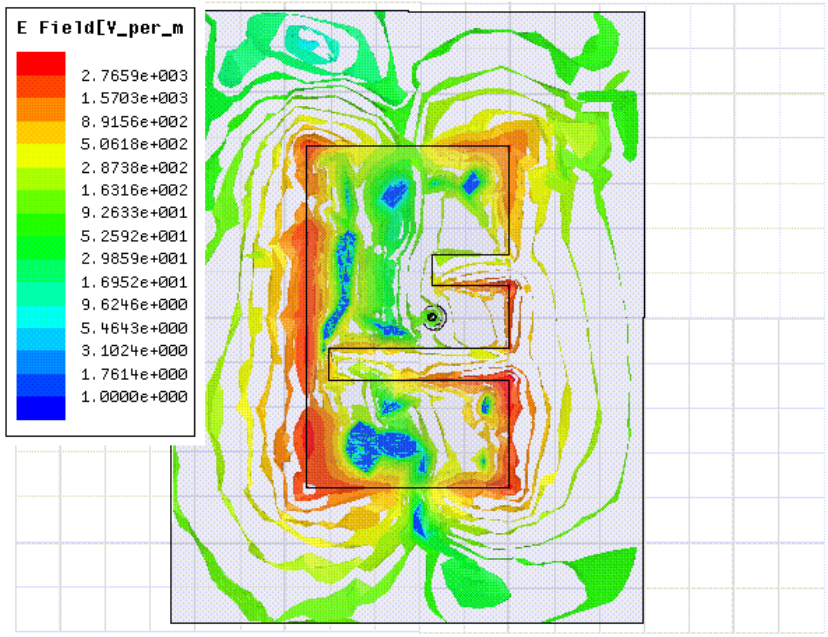

Field distribution beneath the patch

LP vs. CP E-Shaped Patches

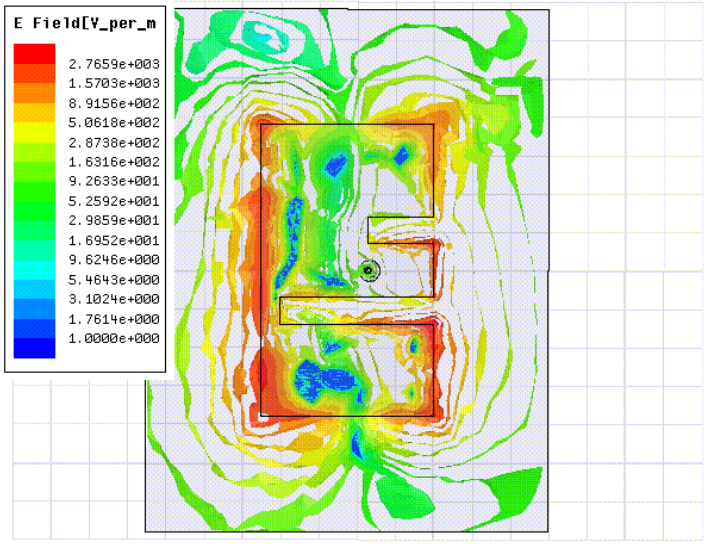

Field distribution beneath the CP E-patch

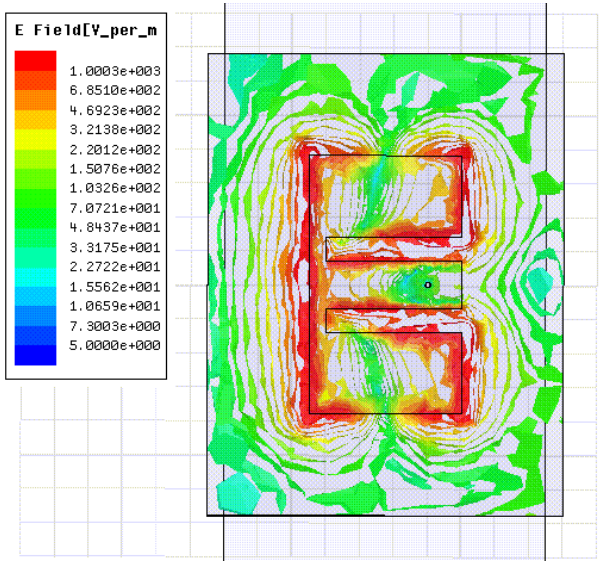

Field distribution beneath the LP E-patch

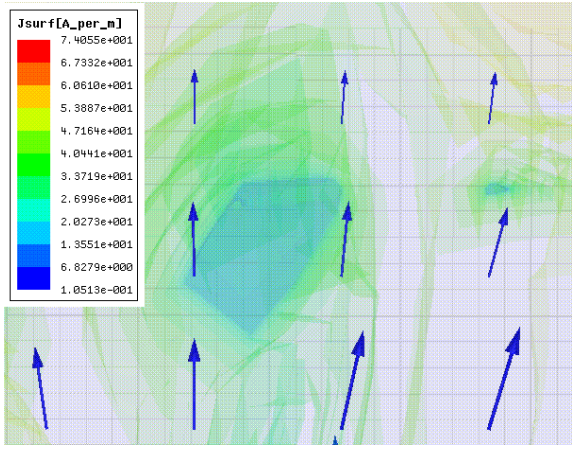

CP Zoomed Current vector distribution

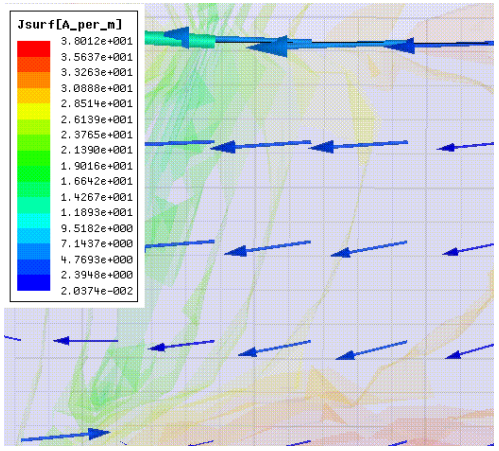

LP Zoomed Current vector distribution

References for circular polarization designs

K. F. Tong, T. P. Wong, "Circularly polarized U-slot antenna," IEEE Trans. Antennas Propagat., Vol. 55, No. 8, pp. 2382-2385, 2007.

S. L. Steven Yang, K. F. Lee, A. A. Kishk and K. M. Luk, "Design and Study of Wideband Single Feed Circularly Polarized Microstrip Antennas", Progress in Electromagnetic Research, vol. 80, pp. 45-61, 2008.

P. Nayeri, K. F. Lee, A. Elsherbeni, F. Yang, "Dual-Band Circularly Polarized Antennas Using Stacked Patches With Asymmetric U-Slots," IEEE Antennas and Wireless Propgation Letters, VOL. 10, pp. 492-495, 2011.

Ahmed Khidre, Kai Fong Lee, Fan Yang, and Atef Elsherbeni, "Wideband Circularly Polarized E-Shaped Patch Antenna for Wireless Applications," IEEE Antennas and Propagation Magazine, Vol. Vol. 52, No.5, pp. 220-229, October 2010.

K. F. Lee, W. C. Mok, K. M. Luk, P. Nayeri, "Single probe-fed circularly polarized patch antennas with U-slots" Microwave and Optical Technology Letters, Vol. 53, No. 6, pp. 1245-1253, 2011.

K. Y. Lam, K. M. Luk, K. F. Lee, H. Wong, K. B. Ng, "Small circularly polarized U-slot wideband patch antenna," IEEE Antenna and Wireless Propagation Letters, Vol. 10, pp. 87-90, 2011.

A. Khidre P. Nayeri Prof. A. Elsherbeni